SIAM J. Applied Dynamical Systems
Vol. 16, No. 1, pp. 91–119

Dynamics of Discrete Time Systems with a Hysteresis Stop Operator*

Maxim Arnold†, Nikita Begun‡, Pavel Gurevich§, Eyram Kwame†, Harbir Lamba¶, and Dmitrii Rachinskii†

Abstract. We consider a piecewise linear two-dimensional dynamical system that couples a linear equation with the so-called a *hysteresis stop* operator. Global dynamics and bifurcations of this system are studied depending on two parameters. More complicated systems involving stop operators may have potential applications in the economic modeling of agents that display frictions and memory dependence.

Key words. stop operator, piecewise linear system, bifurcation, dynamic stochastic general equilibrium model

AMS subject classifications. 37E99, 37E05, 37N40

DOI. 10.1137/16M1073522

1. Introduction.

The *stop* operator was proposed by Prandtl as an elementary model of quasi-static elastoplasticity [49]; see Figure 1(a). It presents a simple example of a *rate-independent* operator with local *memory* [59] and, as such, is used as an elementary building block for important models of *hysteresis* phenomena such as the Prandtl–Ishlinskii operator [35], the Preisach operator [34], and their generalizations [46]. Applications of these *nonsmooth* operators include modeling friction [52], elastoplastic materials [38], magnetic hysteresis [46], fatigue and damage counting [21,53], constitutive laws of *smart* materials [18,29,30], sorption hysteresis [2,10,37,48], and phase transitions [12]. More recent applications range from biology and medicine [23,27] to economics and finance [14,16,36]. On the other hand, a *stop* can also be viewed as a solution operator of a simple variational inequality describing the Moreau sweeping process with rigid characteristic in one dimension [47]; see Figure 1(b).

Modeling of closed systems that exhibit hysteresis typically leads to differential equations which include the above nonsmooth operators. Dynamics of these systems have been ana-

*Received by the editors May 3, 2016; accepted for publication (in revised form) by Jan Sieber October 27, 2016; published electronically January 5, 2017.

http://www.siam.org/journals/siads/16-1/M107352.html

Funding: The second author's work was supported by Saint Petersburg State University (research grant 6.38.223.2014), the Russian Foundation for Basic Research (projects 16-01-00452 and 15-01-03797), and DFG project SFB 910. The work of the third author was supported by the DFG Heisenberg Programme, DFG project SFB 910, and the Ministry of Education and Science of Russian Federation (agreement 02.a03.21.0008). The sixth author's work was supported by NSF grant DMS-1413223.

†University of Texas at Dallas, Richardson, TX 75080 (maxim.arnold@utdallas.edu, exk121230@utdallas.edu, dmitry.rachinskiy@utdallas.edu).

‡Institute of Mathematics, Free University of Berlin, Berlin, 14195, Germany, and Saint Petersburg State University, Russia (nikitabegun88@gmail.com).

§Institute of Mathematics, Free University of Berlin, Berlin, 14195, Germany, and Peoples' Friendship University of Russia, Russia (gurevich@math.fu-berlin.de).

¶Department of Mathematical Sciences, George Mason University, Fairfax, VA 22030 (hlamba@gmu.edu).

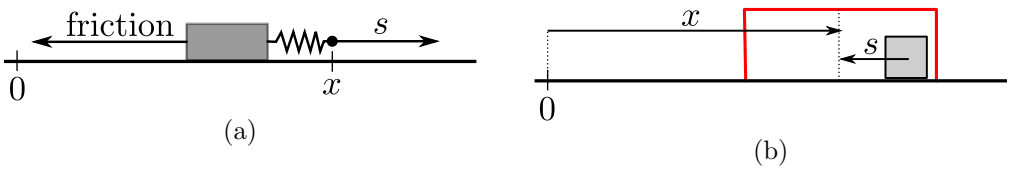

Figure 1. *Interpretations of the stop operator.* (a) *Schematic of Prandtl's model of quasi-static elastoplasticity: the box is not moving unless the absolute value of the force s of the ideal spring reaches the maximal value ρ of friction.* (b) *Schematic of the Moreau sweeping process with rigid characteristic in one dimension. The position x of the center of the outer frame is the input; the relative position s of the center of the frame with respect to the center of the box is the output. The frame moves and drags the box.*

lyzed with various techniques including topological degree methods [3, 5, 11, 33], differential inclusions [40], switched systems [4], and energy considerations using the dissipative property of hysteresis [31]. As most of these models are motivated by engineering and physics applications, they are naturally formulated in a continuous time setting. Discrete time systems with hysteresis operators have received little attention and were studied mostly in the context of numerical discretizations of continuous systems. However, the discrete time modeling is typical for certain applications, e.g., in economics, and one can expect that discrete time models motivated by such applications can exhibit interesting dynamical scenarios when nonsmooth hysteresis terms are included.

In this paper, we consider an example of a simple discrete time system which consists of a linear scalar equation coupled with the one-dimensional *stop* operator. This system can be equivalently written as a two-dimensional piecewise linear map. It has multiple equilibrium points which form a segment in the phase space. We present analysis of global dynamics and bifurcations depending on two parameters. In particular, the global attractor can consist of two semistable equilibrium points, a segment of stable equilibrium points, a segment of unstable equilibrium points, a 2-periodic orbit, a 2-periodic orbit together with two semistable equilibrium points, or, in a critical case, a two-dimensional set of equilibrium and 2-periodic points. For a certain open set of parameter values, the system possesses infinitely many unstable periodic orbits.

The paper is organized as follows. The next section contains the main result. In section 3, we present a motivating discussion including continuous time mechanical systems and discrete time economic models. In particular, in a standard setting of a general equilibrium macroeconomic model, we propose modeling stickiness in an agent's expectations by the *play* operator dual to the *stop*. This leads us to a four-dimensional system containing the *stop* operator, and we present a few numerical examples of its dynamics. The two-dimensional system discussed in section 2 can be considered as a simple prototypical counterpart of this higher-dimensional economic model. Section 4 contains the proofs. Conclusions are presented in the last section.

2. Main results. Let $s_0 \in [-1, 1]$ and let $\{x_n\}$, $n \in \mathbb{N}_0$, be a real-valued sequence. The *stop* operator S maps a pair s_0, $\{x_n\}$ to a sequence defined by the formula

$$s_{n+1} = \Phi(s_n + x_{n+1} - x_n), \quad n \in \mathbb{N}_0,$$

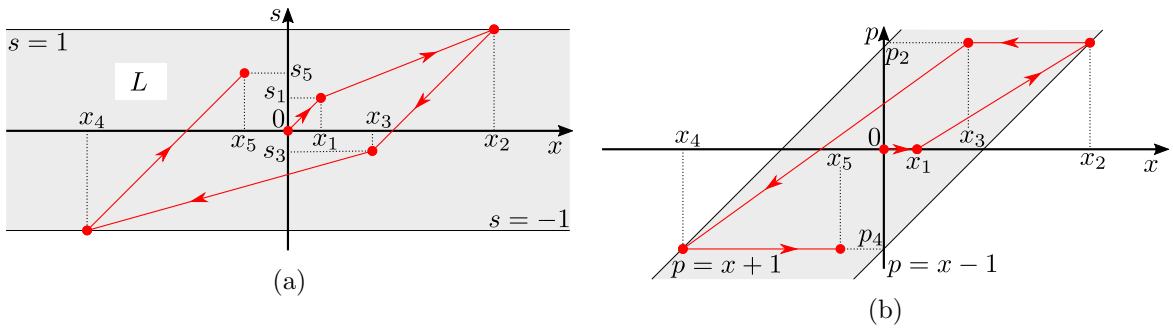

Figure 2. *Interpretations of the stop and play operators.* (a) *An example of the input-output sequence of the stop operator:* $(0,0)=(x_0,s_0)$, (x_1,s_1), $(x_2,1)$, (x_3,s_3), $(x_4,-1)$, (x_5,s_5). (b) *An example of the input-output sequence of the play operator:* $(0,0)=(x_0,p_0)$, (x_1,p_0), (x_2,p_2), (x_3,p_2), (x_4,p_4), (x_5,p_4).

where the piecewise linear saturation function Φ is defined by

$$\Phi(\tau)=\begin{cases} -1 & \text{if} \quad \tau<-1,\\ \tau & \text{if} \quad |\tau|\le 1,\\ 1 & \text{if} \quad \tau>1; \end{cases} \tag{2.1}$$

see Figure 2(a). Here s_0 is called the initial state, $\{x_n\}$ is called the input, and $\{s_n\}$ is called the output (or the variable state) of the stop operator. The operator that maps the pair s_0, $\{x_n\}$ to the sequence $\{p_n\}$ with $p_n=x_n-s_n$ is called the *play* operator (see Figure 2(b)).

Coupling the output of the stop operator with the input sequence via a linear transformation with real-valued coefficients λ and a, we consider the dynamical system

$$\begin{cases} x_{n+1}=\lambda x_n+as_n,\\ s_{n+1}=\Phi(s_n+x_{n+1}-x_n) \end{cases} \tag{2.2}$$

with $n\in\mathbb{N}_0$ on the strip

$$L=\{(x,s): x\in\mathbb{R}, s\in[-1,1]\}. \tag{2.3}$$

From here on we assume that $|\lambda|<1$. This inequality ensures that all the trajectories of system (2.2) are bounded.

It is easy to see that the equilibrium points of system (2.2) form the segment

$$EF=\left\{(x,s):\ x=\frac{as}{1-\lambda},\ -1\le s\le 1\right\} \tag{2.4}$$

with the end points

$$E=(x^*,1)=\left(\frac{a}{1-\lambda},1\right),\quad F=(-x^*,-1)=\left(-\frac{a}{1-\lambda},-1\right). \tag{2.5}$$

We use the standard notion of stability and instability (in the Lyapunov sense) for equilibria and periodic orbits. We will also say that an equilibrium point (x_e,s_e) of system (2.2) is *semistable* if there are open sets $U_1,U_2\subset\{(x,s):|s|<1\}$ such that (x_e,s_e) belongs to their boundaries and simultaneously

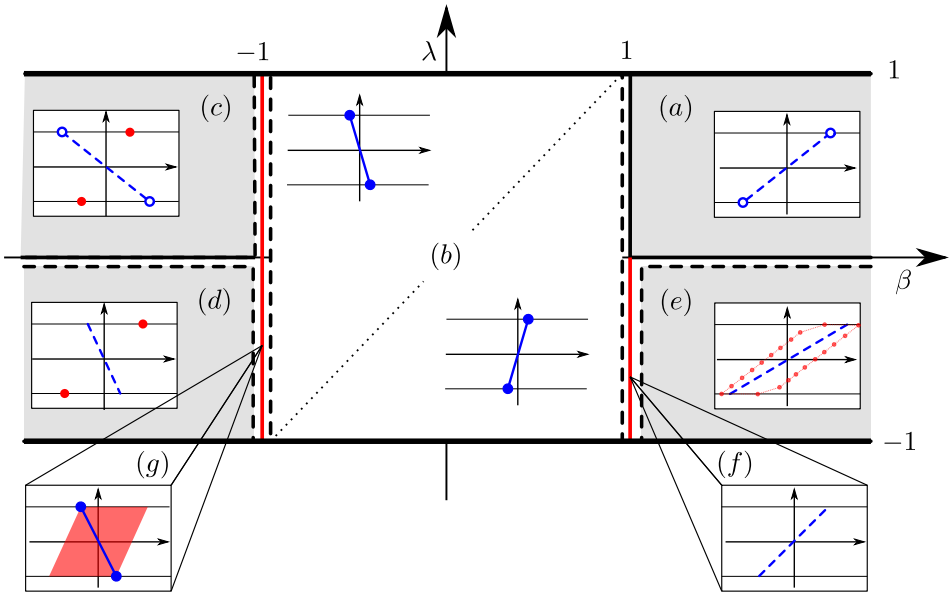

Figure 3. *Bifurcation diagram. The segment EF of the fixed points is shown by a blue line. Stable fixed points are denoted by a solid line; unstable fixed points are shown by a dashed line. Stable end points of EF are shown as filled blue discs; semistable points are denoted by empty blue discs; in the unstable case, no special notation is used. The dotted line in case (b) corresponds to the set of parameters leading to the infinite slope of the line EF. Periodic points are shown in red. Filled red discs in cases (c) and (d) correspond to the stable 2-periodic orbit $\pm Q$; the red parallelogram Σ in case (g) consists of stable 2-periodic orbits. Case (e) corresponds to complex dynamics when the system has periodic orbits with arbitrary large periods (see Theorem 2.2). One such orbit is sketched on the diagram. In the critical case (f), the segment EF attracts all the trajectories.*

- for every $\varepsilon > 0$ there is a $\delta > 0$ such that any trajectory starting from the δ-neighborhood of the equilibrium point (x_e, s_e) in the set U_1 belongs to the ε-neighborhood of (x_e, s_e) for all positive n;
- there is an $\varepsilon_0 > 0$ such that any trajectory starting in U_2 leaves the ε_0-neighborhood of the equilibrium (x_e, s_e) after a finite number of iterations.

Our main result consists in the classification of the long time behavior for the orbits of system (2.2). The dynamics of system (2.2) depends on the values of the parameters λ and $\beta = \lambda + a$ as described in the Theorem 2.1 (see also Figure 3).

Theorem 2.1. *Let $\beta = \lambda + a$ and $|\lambda| < 1$.*

(a) *If $\lambda \geq 0$, $\beta \geq 1$, then the equilibrium points E and F are semistable and all the other equilibrium points are unstable. Each nonequilibrium trajectory converges either to E or to F.*

(b) *If $|\beta| < 1$, then all the equilibrium points are stable and each trajectory of system (2.2) converges to an equilibrium point.*

(c) *If $\lambda \geq 0$, $\beta < -1$, then the points E and F are semistable, all the other equilibrium points are unstable, and there exists a stable 2-periodic orbit*

$$\pm Q = \left(\mp \frac{a}{1+\lambda}, \pm 1 \right). \tag{2.6}$$

Each nonequilibrium trajectory converges either to E or to F or to the orbit (2.6).

(d) *If $\lambda < 0$, $\beta < -1$, then all the equilibrium points are unstable. Each nonequilibrium trajectory converges to the stable 2-periodic orbit (2.6).*

(e) *If $\lambda < 0$, $\beta > 1$, then all the equilibrium points are unstable. System (2.2) has periodic orbits of all sufficiently large periods. At most one periodic orbit is stable.*

(f) *If $\lambda < 0$, $\beta = 1$, then all the equilibrium points are unstable. Each trajectory either ends up at E or at F or converges to the segment EF.*

(g) *If $\beta = -1$, then all the equilibrium points are stable. The parallelogram*

$$\Sigma = \left\{(x,s):\ 2\frac{(1-\lambda)x-a}{1-\lambda+a}+1 \le s \le 2\frac{(1-\lambda)(x-1)}{1-\lambda+a}+1,\ |s|\le 1\right\} \tag{2.7}$$

with the vertices E, F, $Q = (1,1)$ and $-Q = (-1,-1)$ consists of stable 2-periodic orbits and the diagonal EF of fixed points. Every nonequilibrium trajectory converges either to one of the equilibrium points E or F or to a 2-periodic orbit in the parallelogram Σ.

The existence of infinitely many periodic orbits in case (e) may indicate the presence of a global strange attractor or a chaotic attractor coexisting with the stable periodic orbit. More detailed analysis of this case will be a subject of future work.

Theorem 2.1 describes several bifurcation scenarios. In particular, the period doubling scenario (see case (g)) is a type of a border-collision degenerate flip bifurcation, which is typical for piecewise linear systems [22, 24, 43, 55, 56, 57]. Specifics of the realization of this scenario in system (2.2) are dictated by the fact that 2-periodic orbits bifurcate from an interval of fixed points.

Let us consider β as a decreasing bifurcation parameter. When this parameter crosses the value -1, the equilibrium points of the segment EF, which are stable for $\beta \in (-1,1)$ (see case (b)), destabilize and the 2-periodic orbit (2.6) appears away from the segment EF (see cases (c) and (d)). This transition is accompanied by the creation of the parallelogram Σ filled with 2-periodic orbits at the critical value $\beta = -1$ (case (g)). This parallelogram is spanned by the 2-periodic orbit $\pm Q = (\pm 1, \pm 1)$ and the equilibrium points E, F.

Assume that $\lambda < 0$. When the parameter β increases and crosses the value 1, the equilibrium points destabilize and infinitely many periodic orbits appear (see case (e)). Dynamics for the critical value $\beta = 1$ is described by case (f). The following theorem complements case (e) of Theorem 2.1.

Theorem 2.2. *Assume that the conditions of case (e) of Theorem 2.1 hold and hence system (2.2) has infinitely many periodic orbits, of which at most one is stable. Then the relation $(\lambda,\beta) \in \Omega_k$ with*

$$\Omega_k = \left\{(\lambda,\beta):\ \frac{\beta^k-1}{\beta-1} \le -\frac{1}{\lambda} < \beta^k,\ \beta > 1, -\frac{1}{\lambda} > 1\right\}, \tag{2.8}$$

where $k \in \mathbb{N}$, ensures that system (2.2) has a unique stable $(2k+2)$-periodic orbit. If $(\lambda,\beta) \notin \bigcup_{k=1}^{\infty} \Omega_k$, then all the periodic orbits are unstable.

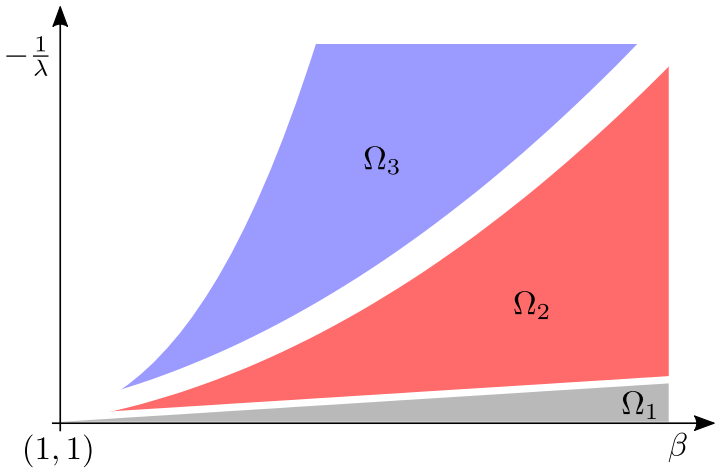

Figure 4. *Domains Ω_k of existence of a (unique) stable periodic orbit of period $2k+2$ in the coordinates $\beta = \lambda + a > 1$ and $-1/\lambda > 1$ for case (e) of Theorem 2.1.*

Remark 1. The domains Ω_k of existence of stable periodic orbits with different periods do not intersect (see Figure 4).

Remark 2. It will follow from the proof of Theorem 2.2 that if (λ, β) belongs to the interior of Ω_k for some k, then the corresponding stable periodic orbit is asymptotically stable.

3. Discussion.

The model (2.2) is of independent mathematical interest as a simply defined discrete time piecewise linear dynamical system. However, in this section we briefly describe its potential relevance to the rigorous modeling of hysteresis in important real-world applications such as mechanical systems and economics. The section can safely be omitted if desired.

3.1. Mechanical systems.

Differential equations involving the stop operator, or multiple stop operators, have been used for modeling mechanical systems with plastic elements or dry friction (see, for example, [1, 28, 39, 51, 60]). The simplest example is an oscillator on an elastic-ideal plastic spring,

$$\ddot{x}(t) + k\dot{x}(t) + s(t) = 0, \qquad s(t) = S[x](t), \tag{3.1}$$

where S is the extension of the stop operator from the space of discrete time inputs $\{x_n\}$ and outputs $\{s_n\}$ to the space of continuous time inputs $x(t) : \mathbb{R}_+ \to \mathbb{R}$ and outputs $s(t) : \mathbb{R}_+ \to \mathbb{R}$ [34, 59]. Using the more complex Prandtl–Ishlinskii model for the stress-strain law of the elasto-plastic spring, or the Maxwell-slip friction model for the dry friction, results in replacing the stop operator in this equation by a weighted sum of multiple stop operators [51, 60]:

$$\ddot{x}(t) + k\dot{x}(t) + \hat{s}(t) = 0, \qquad \hat{s}(t) = \sum_{i=1}^{m} \mu_i S[\rho_i^{-1} x](t), \tag{3.2}$$

where $\mu_i, \rho_i > 0$. In a more general setting, (3.1) and (3.2) represent a wider class of mechanical models, which involve multiple coupled linear and dry friction elements and can be written in the form

$$\dot{z}(t) = \Lambda z(t) + \sum_{i=1}^{m} M_i s^i(t), \qquad s^i(t) = S[u^i](t), \qquad u^i = Q_i^T z, \tag{3.3}$$

where $z \in \mathbb{R}^\ell$, Λ is an $\ell \times \ell$ matrix, and $M_i, Q_i \in \mathbb{R}^\ell$.

System (3.3) motivates our interest in dynamics of its discrete time counterpart

$$z_{n+1} = \Lambda z_n + \sum_{i=1}^{m} M_i s_n^i, \qquad s_{n+1}^i = \Phi\left(s_n^i + Q_i^T(z_{n+1} - z_n)\right). \tag{3.4}$$

In particular, (2.2) is the simplest system of type (3.4). Of course, one might expect that some dynamics of systems (3.3) and (3.4) are similar, while others may be different (specifically, if (3.4) is not a discretization of (3.3)).

3.2. Models of economics. In economics, hysteresis has been well-documented in the relationship between the output of the economy and unemployment rate [6]. Hysteresis is also closely associated with other widely observed phenomena such as *path dependence* [9, 25], *stickiness* of prices and information [7, 20, 45], and *heterostasis* (multiplicity of equilibria) [15] that describe empirical economic data. To explain such empirical observations within, for example, a linear, unique equlibrium, economic model often involves adding a posteriori assumptions such as the existence of an eigenvalue with largest modulus close to, but inside, the unit circle (the unit root hypothesis).

Obtaining quantitative models of these empirical observations naturally motivates the use of the play operator and more complex models of hysteresis developed in physics in the economic context. For example, the play operator was shown to produce a good model of the dependence of supply and demand on the price [8,26]. This model was fitted to microeconomic data based on a survey of German beer exports. It replaced the demand and supply curves by play operators and predicted well the observed price rigidity. Similarly, the Preisach operator has been applied to modeling hysteresis in unemployment [17]. Furthermore, the phenomenology of these hysteresis models is compatible with multiagent modeling frameworks for economic models (for example, [14, 41, 42]).

A next natural step toward modeling the above effects in economics consists of the formulation and analysis of closed models. With this in mind, consider the following example of a (toy) dynamic stochastic general equilibrium (DSGE) model from macroeconomics (see, for example, [13, 32, 50, 58] for different DSGE models):

$$\begin{cases} y_{n+1} = y_n - a_1(v_{n+1} - \sigma_{n+1}) + \varepsilon_n, \\ u_{n+1} = b_1\sigma_{n+1} + (1 - b_1)u_n + b_2 y_{n+1} + \eta_n, \\ v_{n+1} = c_1(u_{n+1} - u^*) + c_2 y_{n+1} + c_3 v_n + \xi_n, \end{cases} \tag{3.5}$$

where y_n is the output gap (or employment rate, or another measure of activity of the economy), u_n is the rate of inflation, v_n is the interest rate, σ_n is the aggregate of the economic

agents' expectation of the future inflation rate, and ε_n, η_n, ξ_n are exogenous noise terms; see [19] for a very similar toy model. All the parameters are nonnegative, $b_1 < 1$, and the parameter u^*, the inflation target, is for convenience set to zero. More complicated variants, employing many more variables to represent different sectors of the economy, are still widely used by central banks to help determine interest rate policy.

In order to close the model, (3.5) must be complemented with an equation defining how the economic agents' expectation of the future inflation rate σ_n is related to the actual inflation rate u_n. In most standard DSGE models the agents are, put very simply, assumed to have rational expectations about the future. However, there is empirical evidence that, in practice, the process of forming inflation expectations displays hysteresis and in particular stickiness in the sense that many agents will update their expectations only infrequently [44]. Evidence such as this has led to the development of a number of simple ad hoc models throughout economics that attempt to account for "boundedly rational" behavior of economic agents caused by their limited access to information, limited cognitive abilities, emotional behavior, and other human factors. One commonly used modeling heuristic is based around the concept of a threshold—it is postulated that an agent changes its behavior (strategy, opinion) when a variable reaches a certain threshold value (see [54], for example). Play operators may provide a useful alternative to such models because they also incorporate threshold effects and are capable of accounting for the path dependence, hysteresis, and multiplicity of equilibrium states in an economic model. At the same time they possess a set of useful and well-understood mathematical properties which facilitate the modeling and analysis.

If we therefore suppose that the expectation of the future inflation rate σ^i by an agent i is related to the actual inflation rate u via a play operator, then

$$\sigma^i_{n+1} = u_{n+1} - \rho_i s^i_{n+1}, \qquad s^i_{n+1} = \Phi\left(s^i_n + \rho_i^{-1}(u_{n+1} - u_n)\right), \tag{3.6}$$

where Φ is function (2.1) (see Figure 2(b)), ρ_i is a positive threshold parameter, and the sequence $\{s^i_n\}$ (for fixed i) is the output of the *stop* operator with input $\{\rho_i^{-1}u_n\}$ (see Figure 2(a)). According to this definition, the expectation of the future inflation rate remains unchanged as long as the actual current inflation rate deviates from the expected value by less than the value ρ_i. In other words, the agent is not responsive to such variations of the inflation rate. However, once the absolute value of the difference between the expected and the actual rates exceeds the threshold ρ_i, that is, $|\sigma^i_{n-1} - u_n| > \rho_i$ at some time n, the agent corrects its expectation of the future rate making sure that $|\sigma^i_n - u_n| \le \rho_i$ at all times. It may be considered as a technical assumption of the model that the agent makes the minimal possible correction which ensures that the error between the expectation and the actual inflation rate never exceeds the threshold ρ_i, that is, $\sigma^i_n = u_n - \rho_i$ if $u_n > \sigma^i_{n-1} + \rho_i$ and $\sigma^i_n = u_n + \rho_i$ if $u_n < \sigma^i_{n-1} - \rho_i$. This rule is similar to some trading strategies based on draw-up and draw-down indicators that are used by momentum traders in financial markets [36].

The aggregate of economic agents' expectation of future inflation rate σ_n in the macroeconomic model (3.5) can be naturally defined as

$$\sigma_n = \sum_{i=1}^{m} \mu_i \sigma^i_n \tag{3.7}$$

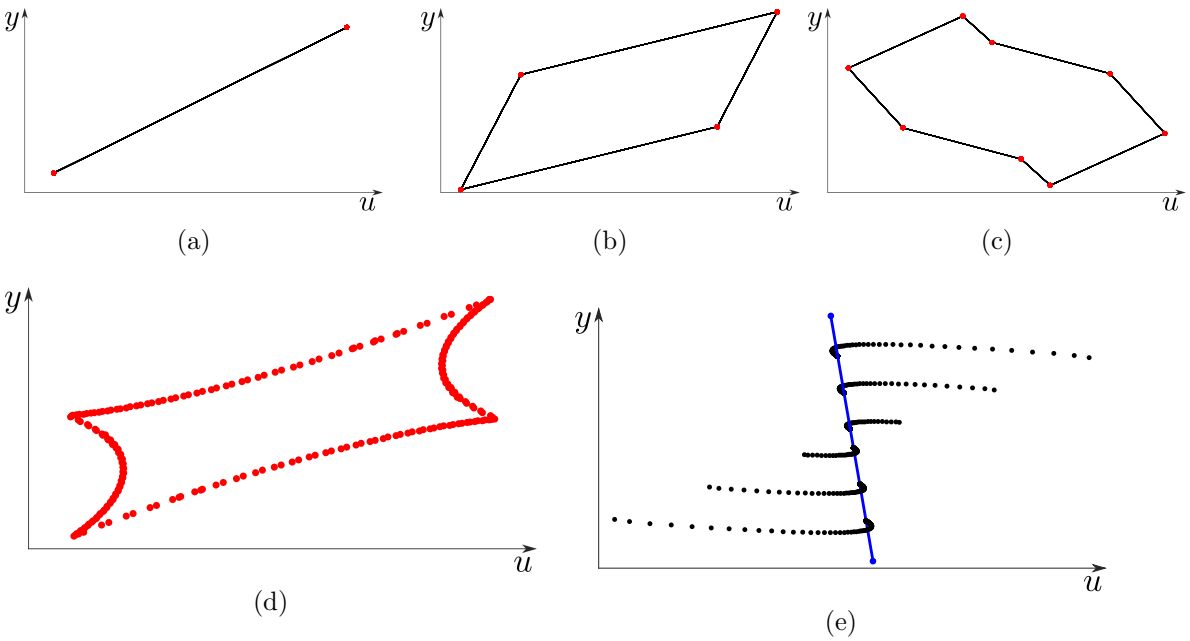

Figure 5. *Projections of various trajectories of system* (3.5)–(3.7) *onto the* (u, y) *plane. The noise terms in* (3.5) *are zero. The system contains one stop operator (one representative agent), that is,* $m = 1$, $\rho_1 = 1$, $\mu_1 = 1$. *Parameters of* (3.5) *are given in the format* a_1, $b = (b_1, b_2)$, $c = (c_1, c_2, c_3)$. (a) 2*-periodic orbit for* $a_1 = 0.99$, $b = (0.76, 0.9)$, $c = (1.4, 9.7, 0.025)$. (b) 4*-periodic orbit for* $a_1 = 0.7$, $b = (0.75, 0.5)$, $c = (4.8, 3.6, 3.45)$. (c) 8*-periodic orbit for* $a_1 = 0.9$, $b = (0.73, 0.9)$, $c = (1.2, 3.15, 1.3)$. (d) *Quasi-periodic orbit for* $a_1 = 0.7$, $b = (0.7, 0.55)$, $c = (4.8, 4.15, 3.8)$. (e) *Trajectories converging to different points of the segment of equilibrium points for* $a_1 = 0.01$, $b = (0.01, 0.03)$, $c = (1, 6, 0.54)$. *Similar results have been obtained in the model with multiple stop operators representing agents with different thresholds.*

in a model with m agents, which have different thresholds ρ_i and contribute to the aggregate with weights $\mu_1, \dots, \mu_m > 0$. Equations (3.5) complemented by relations (3.6) and (3.7) form a closed economic model with m stop operators.

If we set the noise terms ε_n, η_n, ξ_n in (3.5)–(3.7) to zero, then the resulting autonomous system can be rewritten in the explicit form (3.4) with $z = (y, u, v)^T \in \mathbb{R}^3$ and a 3×3 matrix Λ. Figure 5 presents various attractors of this model obtained numerically for different parameter regimes. In particular, trajectories can converge to stable equilibrium points that form a segment in the phase space; see Figure 5(e). Alternatively, one can observe convergence to a 2-periodic orbit, or to a periodic orbit of a higher period, which coexists with the set of unstable equilibrium points (see Figures 5(a)–(c)). Figure 5(d) demonstrates the possibility of quasi-periodic dynamics. Comparing these scenarios with different cases of Theorem 2.1 suggests that the prototype model (2.2) can help us understand some features of dynamics of higher-dimensional models (3.4) (although it should be pointed out that many of the parameter regimes we shall study will not be economically plausible).

4. Proofs.

We will prove statements of Theorem 2.1 in the counterclockwise order along the bifurcation diagram in Figure 3. Thus, we prove case (a) in section 4.1, then case (b) for nonnegative λ in section 4.2. Proofs for cases (c) and (d) are presented in sections 4.3 and

section 4.4, respectively. In section 4.5, we present the proof of the remaining part of case (b) for negative λ. Proofs of case (e) and of Theorem 2.2 are presented in section 4.6. Finally, sections 4.7 and 4.8 contain the proofs for critical cases (f) and (g), respectively.

We use the following notation: A_x and A_s will denote the x and s coordinates of a point A in the (x,s)-plane. Transformation (2.2) of strip $L \subset \mathbb{R}^2$ (see (2.3)) into itself will be denoted by f. Throughout the proofs, we will use the variable $p = x - s$ (output of the play operator; see Figure 2(b)). We will denote by $A_p = A_x - A_s$ the p-coordinate of a point A.

Let us start with a few auxiliary lemmas. Due to the fact that

$$f(-x,-s) = -f(x,s), \tag{4.1}$$

it is sufficient to present the proofs for only half of the phase space.

Lemma 4.1. *For any point A to the left of the segment EF, one has $[f(A)]_x > A_x$. For any point B to the right of the segment EF, one has $[f(B)]_x < B_x$.*

Proof. Since A lies to the left of the segment EF, one has $(1-\lambda)A_x < aA_s$. Thus $[f(A)]_x = \lambda A_x + aA_s > \lambda A_x + (1-\lambda)A_x = A_x$. The second statement follows from (4.1). ∎

Lemma 4.2. *Let $\beta > 0$. Then for any two points A and B with the same p-coordinate $A_p = B_p$, from $A_x > B_x$ it follows $[f(A)]_x > [f(B)]_x$.*

Proof. It suffices to note that $[f(A)]_x = \lambda A_x + aA_s = \beta A_x - aA_p$. ∎

Denote by $\Pi \subset L$ the parallelogram with the diagonal EF, two sides on the lines $s = \pm 1$, and two sides with slope 1 (see Figure 7 later):

$$\Pi = \left\{ (x,s) : \ |x-s| \le \left| \frac{a}{1-\lambda} - 1 \right|, \ |s| \le 1 \right\}. \tag{4.2}$$

Lemma 4.3. *Let $(x_0,s_0) \in \Pi$ and $p_0 = x_0 - s_0$. If either $-1 < \beta < 0$ and $|\beta x_0 - (a+1)p_0| \le 1$ or $0 \le \beta < 1$, then the trajectory with the initial point (x_0,s_0) satisfies $p_n = p_0$ for all $n \ge 0$ and $(x_n,s_n) \to (x_*,s_*)$ as $n \to \infty$, where*

$$(x_*,s_*) = \Big(-\frac{ap_0}{1-\beta}, -\frac{(1-\lambda)p_0}{1-\beta} \Big) \tag{4.3}$$

is a fixed point of f with $x_* - s_* = p_0$.

Proof. Consider a sequence (x_n,s_n) defined by

$$x_{n+1} = \beta x_n + a(s_n - x_n), \qquad s_{n+1} = x_{n+1} - x_n + s_n \tag{4.4}$$

and suppose that $|s_n| \le 1$ for all n. Then, according to (2.1), this sequence is a trajectory of (2.2). Equations (4.4) are equivalent to the relations $x_n - s_n = p_0$, $x_{n+1} = \beta x_n - ap_0$, which results in the explicit formulas

$$x_n - x_* = s_n - s_* = \beta^n (x_0 - x_*) = \beta^n (s_0 - s_*), \tag{4.5}$$

where we use the notation (4.3). Since $s_0, s_* \in [-1,1]$, (4.5) implies $|s_n| \le 1$ for all n if $0 \le \beta < 1$. Similarly, if $-1 < \beta < 0$ and, in addition, $|s_* + \beta(s_0 - s_*)| \le 1$, then (4.5) also

implies $|s_n| \le 1$ for all n. By the definition of s_*, we have $s_* + \beta(s_0 - s_*) = \beta x_0 - (a+1)p_0$, hence under the assumptions of the lemma, the sequence s_n defined by (4.5) satisfies $|s_n| \le 1$, and therefore formulas (4.5) explicitly define a trajectory of (2.2). It remains to note that from (4.5), it follows that $x_n - s_n = x_* - s_* = p_0$ and $x_n \to x_*, s_n \to s_*$ for $|\beta| < 1$. ∎

Lemma 4.4. *For $0 \le \lambda < 1$, $\beta \le 0$ and for $-1 < \lambda \le 0$, $-1 \le \beta \le 0$ the parallelogram Π is invariant under the map (2.2).*

Proof. Let $(x_n, s_n) \in \Pi$, i.e., $|p_n| \le \frac{1-\beta}{1-\lambda}$. If $0 \le \lambda < 1$, $\beta \le 0$, then

$$|x_{n+1}| \le \lambda \frac{1-\beta}{1-\lambda} - \beta = -\frac{a}{1-\lambda},$$

hence

$$|x_{n+1}| \le -\frac{a}{1-\lambda} + 2. \tag{4.6}$$

If $-1 < \lambda \le 0$, $-1 \le \beta \le 0$, then

$$|x_{n+1}| \le -\lambda \frac{1-\beta}{1-\lambda} - \beta,$$

which, again, yields (4.6) because $\lambda < 1$ and $\lambda\beta \le 1$.

Using the definition (2.1) of the saturation function Φ, from the second equation of system (2.2) one can see that

$$p_{n+1} = p_n \ \text{ if } \ |s_{n+1}| < 1; \quad p_{n+1} \ge p_n \ \text{ if } \ s_{n+1} = 1; \quad p_{n+1} \le p_n \ \text{ if } \ s_{n+1} = -1.$$

Combining these relations with (4.6), we obtain

$$p_{n+1} = p_n \ \text{ if } \ |s_{n+1}| < 1; \ \ p_n \le p_{n+1} \le \frac{1-\beta}{1-\lambda} \ \text{ if } \ s_{n+1} = 1; \ \ \frac{\beta-1}{1-\lambda} \le p_{n+1} \le p_n \ \text{ if } \ s_{n+1} = -1.$$

Hence, the relation $|p_n| \le \frac{1-\beta}{1-\lambda}$ always implies $|p_{n+1}| \le \frac{1-\beta}{1-\lambda}$, which is equivalent to the implication $(x_n, s_n) \in \Pi \ \Rightarrow \ (x_{n+1}, s_{n+1}) \in \Pi$. ∎

Lemma 4.5. *System (2.2) has a 2-periodic orbit if and only if $\beta \le -1$. If $\beta < -1$, then a 2-periodic orbit is unique and consists of the point $\pm Q$ defined by (2.6).*

Proof. A 2-periodic orbit $A_1 = (x_1^*, s_1^*)$, $A_2 = f(A_1) = (x_2^*, s_2^*)$ of (2.2) satisfies

$$x_1^* = \lambda x_2^* + a s_2^*, \qquad x_2^* = \lambda x_1^* + a s_1^*, \tag{4.7}$$

where we assume without loss of generality that $s_1^* \le s_2^*$. It follows from the definition of the stop operator that if the input sequence x_n and the output sequences s_n of this operator are 2-periodic, then either $x_n - s_n = \text{const}$ or s_n alternates between the values ± 1. Hence, the same is true for a 2-periodic orbit, i.e., either $x_1^* - x_2^* = s_1^* - s_2^*$ or $s_1^* = -s_2^* = -1$. In the former case, dividing the difference of (4.7) by $x_1^* - x_2^*$ gives $\beta = -1$, and conversely, it is straightforward to check that if $\beta = -1$, then all points of the parallelogram (2.7) except for the diagonal EF

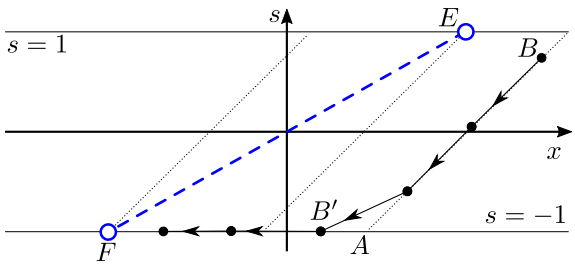

Figure 6. $\lambda \geq 0$, $\beta \geq 1$. *A trajectory starting at a point B to the right of the segment EF converges to the fixed point F. Dotted lines have slope* 1.

are 2-periodic (see case (g) of Theorem 2.1). In the latter case $s_1^* = -s_2^* = -1$, formulas (4.7) imply

$$x_1^* = -x_2^* = \frac{a}{1+\lambda},$$

i.e., points A_1, A_2 coincide with (2.6). The equality $A_2 = f(A_1)$ is ensured by formulas (4.7) and, additionally, the relations $s_2^* = \Phi(x_2^* - x_1^* + s_1^*)$, $s_1^* = \Phi(x_1^* - x_2^* + s_2^*)$, which due to $A_1 = Q$, $A_2 = -Q$ are equivalent to

$$1 = \Phi\Big(-1 - \frac{2a}{1+\lambda}\Big).$$

This last equation is equivalent to $\beta \leq -1$. ∎

4.1. Case (a). In this case, $\lambda \geq 0$ and $\beta \geq 1$. Therefore $a > 0$ and the slope of the segment EF of equilibrium points is positive and less than or equal to 1 as shown in Figure 6.

Consider a point B which lies to the right of the segment EF. Denote by A the intersection point of the lines $p = B_p$ and $s = -1$. Let B' denote the point at which the trajectory $\{f^n(B)\}$ hits the line $s = -1$ for the first time. From Lemma 4.1 it follows that $[f^{-1}(B')]_x > A_x$, and $[f(A)]_x > F_x$ since $\lambda > 0$. Thus, from Lemma 4.2 we obtain $B'_x > F_x$. Since $B'_s = F_s = -1$, and F is a fixed point, it follows that

$$[f(B')]_x - F_x = (\lambda B'_x - a) - (\lambda F_x - a) = \lambda(B'_x - F_x).$$

Hence, due to $\lambda \in [0, 1)$, the trajectory converges to the equilibrium F along the line $s = -1$ (see Figure 6). We conclude that every trajectory that starts to the right of the segment EF of equilibrium points, converges to F. Every trajectory which starts to the left of EF converges to E due to (4.1).

4.2. Case (b), $\lambda \geq 0$.

4.2.1. $0 < \beta < 1$. In this case, the segment EF has a positive slope greater than 1 if $a > 0$ and nonpositive if $a \leq 0$.

1. First, let us consider the trajectory of a point A that belongs to the parallelogram Π defined by (4.2); see Figure 7. Then, by Lemma 4.3, this trajectory converges to the fixed point P^*, which lies at the intersection of the line $p = A_p$ with the segment EF.

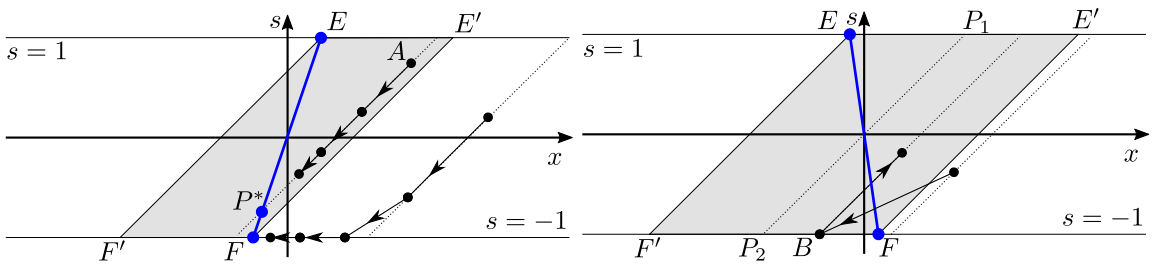

(a) $0 < \beta < 1$. (b) $-1 < \beta \le 0$.

Figure 7. *Theorem* 2.1(b). *Case* $\lambda \ge 0$. *Dotted lines have slope* 1. *The shaded area is the parallelogram* $\Pi = EE'FF'$.

2. Thanks to Lemma 4.2, all the other trajectories that start to the right of the parallelogram Π move down along the line $p = \text{const}$ until they hit the line $s = -1$ and then monotonically converge to the equilibrium point F along this line from the right; see Figure 7(a).

4.2.2. $-1 < \beta \le 0$. In this case, $a < 0$ and the segment EF has a negative slope as in Figure 7(b).

1. If a trajectory starts to the right of the parallelogram Π, then, since $\beta \le 0$, it hits the line $s = -1$ after one iteration. If it hits the line to the right of the equilibrium F, then the trajectory converges to this equilibrium along the line $s = -1$ from the right due to $\lambda \ge 0$. On the other hand, if this trajectory hits the line $s = -1$ at a point B to the left of the point F, then B belongs to the parallelogram Π. In order to show this, we note that for the previous point $f^{-1}(B) = (x_n, s_n)$, we have

$$x_n - s_n > -\frac{a}{1-\lambda} + 1,$$

because the point (x_n, s_n) lies to the right of the parallelogram Π. Therefore,

$$\begin{aligned} x_{n+1} = \lambda x_n + a s_n &> \lambda\left(-\frac{a}{1-\lambda} + 1 + s_n\right) + a s_n \\ &\ge \lambda\left(-\frac{a}{1-\lambda} + 1\right) + \lambda + a. \end{aligned}$$

This last expression is greater than $F'_x = \frac{a}{1-\lambda} - 2$, which is the x-coordinate of the lower left vertex of the parallelogram Π.

2. Consider points on the horizontal sides of Π. To be definite, assume that $s_n = -1$. Denote by $P_1 = (1, 1)$ and $P_2 = (-1, -1)$ the middle points of EE' and FF', respectively. If $(x_n, s_n) \in P_2F$, then the conditions of Lemma 4.3 are satisfied, and the trajectory converges to the equilibrium along the line $p = \text{const}$. Let $(x_n, s_n) \in F'P_2$. If $s_{n+1} < 1$, then, again using Lemma 4.3, the trajectory converges to the equilibrium along the line $p = \text{const}$. If $s_{n+1} = 1$, then $(x_{n+1}, s_{n+1}) \in EP_1$ because $x_{n+1} = \lambda x_n - a \le -\lambda - a < 1$. Since the segments EP_1 and P_2F are centrally symmetric, and the function f is odd, this trajectory also converges to the equilibrium along the line $p = \text{const}$.

It remains to consider points in Π that belong to the open band $|s| < 1$. A trajectory starting from such a point either converges to an equilibrium along the line $p = \text{const}$ without hitting the lines $s = \pm 1$ or hits one of these lines and then converges to an equilibrium as discussed above.

4.3. Case (c). As in the previous case, $a < 0$ and the segment EF has a negative slope (see Figure 8). In this case, by Lemma 4.5, there is a unique 2-periodic orbit consisting of the points $\pm Q$ defined by (2.6).

Now we consider dynamics of trajectories starting in different parts of the phase space.

4.3.1. Invariant segment AB for f^2. Denote

$$A = \left(\frac{a+2}{1-\lambda}, 1\right), \quad B = \left(\frac{1}{\lambda}\left(-\frac{a+2}{1-\lambda} - a\right), 1\right). \tag{4.8}$$

If $\lambda = 0$, we formally set $B_x = \infty$ and replace the segment AB below by the corresponding half-line. Note that $B_x > A_x$ and $Q \in AB$.

The following lemma ensures that if the point B lies to the right of the point E', then any trajectory starting from the segment AE' converges to a 2-periodic orbit.

Lemma 4.6. *Under the hypothesis of Theorem 2.1(c), the segment AB is invariant under the second iteration f^2 of the map f and f^2 is a contraction on AB.*

Proof. First, we note that if a point (x_n, s_n) lies on the line $s = 1$ to the right of the point A, then the image $(x_{n+1}, s_{n+1}) = f(x_n, s_n)$ of this point under the map (2.2) belongs to the line $s = -1$. Indeed,

$$x_{n+1} - x_n = \lambda x_n + a - x_n \le (\lambda - 1)A_x + a = -2,$$

which implies $s_{n+1} = -1$. By (4.1), the points of the line $s = -1$ lying to the left of $-A$ are mapped to the line $s = 1$. Furthermore, if a point (x_n, s_n) lies on the line $s = 1$ between the points A and B, then its image $f(x_n, s_n) = (\lambda x_n + a, s_{n+1})$ lies on the line $s = -1$ to the left of the point $-A$, and therefore the second iteration $f^2(x_n, s_n)$ belongs to the line $s = 1$. Hence, the segment AB is mapped by the second iteration f^2 to the line $s = 1$. Therefore, it remains to show that the scalar function $\phi(y) = [f^2(y, 1)]_x$ maps the interval $[A_x, B_x] \ni y$ into itself and is a contraction on this interval. To this end, note that $\phi(y) = \lambda^2 y + \lambda a - a$ on $[A_x, B_x]$, that is, ϕ is a linear function with the positive coefficient $\lambda^2 < 1$. Thus, we just need to check that $A_x \le \phi(A_x)$ and $\phi(B_x) \le B_x$. Indeed, since

$$\phi(A_x) = \frac{-a + 2\lambda^2 + 2a\lambda}{1-\lambda},$$

the inequality

$$\frac{-a + 2\lambda^2 + 2a\lambda}{1-\lambda} > \frac{a+2}{1-\lambda},$$

which is equivalent to $(\lambda - 1)(\beta + 1) > 0$, ensures that $A_x < \phi(A_x)$. To show that $\phi(B_x) \le B_x$, it is sufficient to establish the following inequality:

$$\lambda^2\left(\frac{-2a - 2 + a\lambda}{\lambda(1-\lambda)}\right) + a(\lambda - 1) < \frac{-2a - 2 + a\lambda}{\lambda(1-\lambda)}.$$

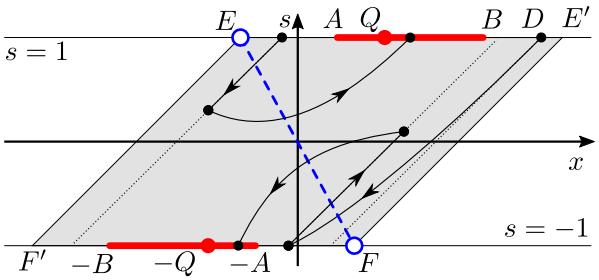

Figure 8. *Case $\lambda \geq 0$, $\beta < -1$. Each of the red segments AB and $-AB$ is mapped into itself by f^2.*

After a simple manipulation, this inequality follows from $\beta + 1 < 0$. ■

4.3.2. Trajectories starting at the segment BE'. Next, we consider the situation when B lies between the points A and E'. Let a trajectory start on the upper side of the parallelogram Π to the right of the point B at a point $D = (x_n, 1)$; see Figure 8. The image $f(D) = (x_{n+1}, -1)$ of this point lies on the line $s = -1$ to the right of the point $-A$. Therefore, $f^2(D)$ belong to the interior of the strip L. Since $\beta < -1$, further iterations $f^{n+k}(D)$ belong to the line $s = -1$ for odd k and to the interior of L for even k, and the x-coordinate of the odd iterations monotonically decreases until the trajectory reaches the half-line $\{(x, s) : x \leq -A_x,\ s = -1\}$. Without loss of generality, we can assume that $f(D)$ is the last point of the trajectory, which is still to the right of the point $-A$ on the line $s = -1$. Let us show that the point $(x_{n+3}, -1)$ lies to the right of the point $(\frac{a}{1+\lambda}, -1)$. To this end, we note that

$$(x_{n+2}, s_{n+2}) = (\lambda x_{n+1} - a, -1 + \lambda x_{n+1} - a - x_{n+1}),$$
$$x_{n+3} = \lambda^2 x_{n+1} - \lambda a + a(-1 + \lambda x_{n+1} - a - x_{n+1}).$$

Thus, we need to show that $x_{n+1} > -\frac{a+2}{1-\lambda}$ implies

$$\lambda^2 x_{n+1} - \lambda a + a(-1 + \lambda x_{n+1} - a - x_{n+1}) > \frac{a}{1+\lambda}, \tag{4.9}$$

i.e.,

$$(\lambda^2 + a\lambda - a)x_{n+1} - a(\beta + 1) > \frac{a}{1+\lambda}.$$

Since $\lambda^2 + a\lambda - a > 1$, it suffices to show (4.9) for $x_{n+1} = -\frac{a+2}{1-\lambda}$, i.e.,

$$(\lambda^2 + a\lambda - a)\left(-\frac{a+2}{1-\lambda}\right) - a(\beta + 1) > \frac{a}{1+\lambda}.$$

But this is equivalent to

$$\lambda^2(\beta + 1) < 0,$$

which is true in the case we are considering. We see that the point $(x_{n+3}, -1)$ belongs to the segment connecting the points $-A$ and $-B$, which is invariant for the map f^2 thanks to Lemma 4.6. Hence the trajectory converges to the 2-periodic orbit.

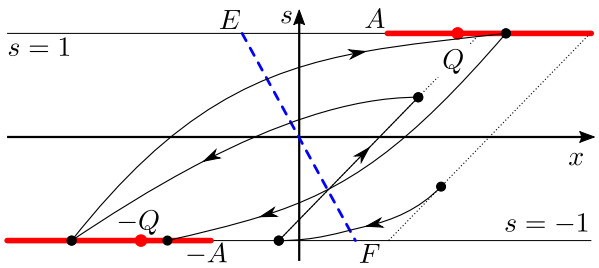

Figure 9. *Case $\lambda < 0$, $\beta < -1$. Red half-lines are mapped to themselves by f^2.*

4.3.3. Trajectories starting at the segment EA. Now, we consider a trajectory which starts at a point D' on the line $s = 1$ to the left of the point A in the parallelogram Π. For this trajectory, further odd iterations $f^k(D')$ lie in the interior of L, while the even iterations $f^k(D')$ belong to the line $s = 1$, and the x-coordinate of the even iterations monotonically increases until the trajectory reaches the segment AB. (This is similar to the behavior that we considered in paragraph 2 in section 4.2.2). Hence, such a trajectory also converges to the 2-periodic orbit.

The above cases cover all the initial conditions from the upper side EE' of Π. Since the map f is odd, trajectories starting at the lower side $F'F$ have similar behavior.

4.3.4. Trajectories starting inside Π. Any trajectory that starts in the parallelogram Π, but not on the lines $s = \pm 1$ and not on the segment of equilibrium points, thanks to Lemma 4.4 will stay inside Π. It reaches one of the lines $s = \pm 1$ in several iterations due to the condition $\beta < -1$. Thus, we see that all the trajectories that start in the parallelogram Π except for the segment of equilibrium points, converge to the 2-periodic orbit.

4.3.5. Trajectories starting outside Π. Finally, let us consider a trajectory that starts to the right of the parallelogram Π. Since $\beta < -1$, this trajectory reaches the line $s = -1$ after one iteration. If it reaches this line to the right of the equilibrium point F, then it will move to the left along the line $s = -1$ and converge to the equilibrium point F from the right. On the other hand, if a trajectory reaches the line $s = -1$ at a point which lies to the left of the point F, then this point belongs to Π. This can be shown exactly in the same way as we did in section 4.2.2. Therefore, such a trajectory converges to the 2-periodic orbit. We conclude that the 2-periodic orbit is stable and its basin of attraction contains the parallelogram Π with the exception of equilibrium points. However, some trajectories from outside the parallelogram Π are attracted to the semistable equilibrium points E and F.

4.4. Case (d). In this case, $a < 0$ and the segment EF has a negative slope (see Figure 9). As in section 4.3, there exists a 2-periodic orbit $\pm Q$ defined by (2.6). Let A be as in (4.8).

First, we note that if a point $(x_n, -1)$ satisfies $x_n \le -A_x$, then $x_{n+1} > \frac{a+2}{1-\lambda}$, $s_{n+1} = 1$. Hence the half-line $\{(x, s) : x \le -A_x, s = -1\}$ is mapped to itself under f^2. Since $x_{n+2} = \lambda^2 x_n - \lambda a + a$ and $\lambda^2 < 1$, any trajectory starting at this half-line converges to the 2-periodic orbit $\pm Q$.

If a point belongs to the open segment $\{(x, s) : -A_x < x < \frac{-a}{1-\lambda}, s = -1\}$, then its trajectory enters the half-line $\{(x, s) : x \le -A_x, s = -1\}$ after finitely many iterations

because $\beta < -1$ (as in section 4.3). Hence, the half-line $\{(x,s) : x < \frac{-a}{1-\lambda},\ s = -1\}$ belongs to the basin of attraction of the 2-periodic orbit. If a point belongs to the half-line $\{(x,s) : x > \frac{-a}{1-\lambda},\ s = -1\}$, then its first iteration is in the half-line $\{(x,s) : x < \frac{-a}{1-\lambda},\ s = -1\}$ because $\lambda < 0$. Hence, we conclude that the lines $s = -1$ and $s = 1$ (except for the equilibria F and E, respectively) belong to the basin of attraction of the 2-periodic orbit.

Finally, all trajectories that start inside the strip $-1 < s < 1$, except for the equilibrium points, will reach one of the lines $s = \pm 1$ after finitely many iterations because $\beta < -1$. Therefore, the 2-periodic orbit attracts all the trajectories except for the equilibrium points and their preimages under the iterations f^k of the map f.

4.5. Case (b), $\lambda < 0$.

4.5.1. $-1 < \beta < 0$. For the point (x_n, s_n) to the right of the parallelogram Π, one has

$$x_n - s_n > p^* = 1 - x^* = 1 - \frac{a}{1-\lambda},$$

and so $x_{n+1} < \lambda p^* - \beta = -x^*$, hence the point (x_{n+1}, s_{n+1}) lies to the left of the equilibrium F on the line $s = -1$; see Figure 10(a). Due to (4.1), for the point (x_n, s_n) to the left of Π, its image will lie on the line $s = 1$ to the right of the point E.

Now, we prove that every trajectory enters Π. Arguing by contradiction, let us show that if a trajectory never entered Π, then the distance from the trajectory to Π would exponentially decrease. This would imply that such a trajectory converges to a 2-periodic orbit, because, as we have seen, its points belong to the union of the lines $s = \pm 1$ and the sign of s_n alternates at every iteration. However, this is impossible as a 2-periodic orbit does not exist in the case we are considering due to Lemma 4.5.

In order to see that the distance from a trajectory to Π exponentially decreases, it is sufficient to establish the inequality

$$q\left(\frac{a}{1-\lambda} - 2 - x_n\right) > \lambda x_n - a + \frac{a}{1-\lambda} - 2$$

for $x_n < \frac{a}{1-\lambda} - 2$ and some $q \in (-\lambda, 1)$ independent of n. This inequality can be written as

$$x_n < \frac{a - (\frac{a}{1-\lambda} - 2)(1-q)}{q+\lambda}.$$

Thus we need to show that

$$\frac{a}{1-\lambda} - 2 < \frac{a - (\frac{a}{1-\lambda} - 2)(1-q)}{q+\lambda},$$

which is equivalent to $(1+\lambda)(\frac{a}{1-\lambda} - 2) < a$ and, further, to $\beta\lambda < 1$. Since the last inequality is true in the case being considered, we can use any $q \in (-\lambda, 1)$. The above argument shows that every trajectory enters the parallelogram Π.

Since $\beta \in (-1, 0)$ and $\lambda \in (-1, 0)$, it follows from Lemma 4.4 that Π is invariant for the map f. Further, we note that if some iteration of a point from Π is mapped in the interior of L, then the trajectory converges to an equilibrium due to $|\beta| < 1$; see Figure 10(a).

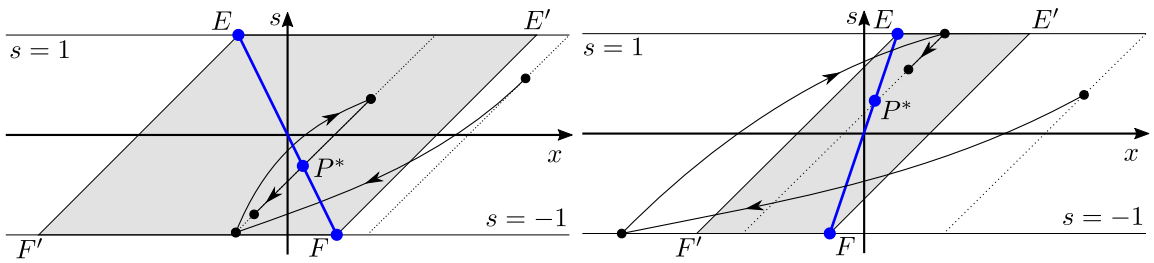

(a) $-1 < \beta < 0$. (b) $0 \le \beta < 1$.

Figure 10. *Theorem* 2.1(b). *Case* $\lambda < 0$.

Finally, let us show that a trajectory cannot jump from the line $s = 1$ to the line $s = -1$ and back indefinitely. Indeed, if this was the case, then a point $(x_n, 1)$ from this trajectory would satisfy $x_n > 1$ and the point $(x_{n+1}, -1)$ would satisfy $x_{n+1} = \lambda x_n + a < -1$. But inequalities $-1 < \beta$ and $x_n > 1$ imply that $-1 - (\lambda x_n + a) < x_n - 1$. In other words, $0 < -1 - x_{n+1} < x_n - 1$ and, similarly, $0 < x_{n+2} - 1 < -1 - x_{n+1}$. Therefore, this trajectory would converge to the 2-periodic orbit, which does not exist in this case due to Lemma 4.5. This contradiction implies that every trajectory converges to an equilibrium point.

4.5.2. $0 \le \beta < 1$. In this case, $a > 0$ and so the slope of the segment EF is greater than 1 (see Figure 10b). If a trajectory starts in Π, then it converges to an equilibrium point $P^* \in EF$ along the line $p = \text{const}$.

A trajectory starting to the right of the parallelogram Π moves along the line $p = \text{const}$ down and left until it reaches the line $s = -1$. At this point, or at the next iteration step, the trajectory reaches a point $(x_n, -1)$ that lies to the left of the equilibrium point F because $\lambda < 0$. If $(x_n, -1) \in \Pi$, then the trajectory converges to an equilibrium due to Lemma 4.3. If the point $(x_n, -1)$ lies to the left of the parallelogram Π, then let us show that the absolute value $|x_n - s_n| = -1 - x_n$ of the p-coordinate of this point is less than the absolute value $|x_{n-1} - s_{n-1}| = x_{n-1} - s_{n-1}$ of the p-coordinate of its preimage (x_{n-1}, s_{n-1}). Moreover, we want to show that $|x_n - s_n| < q|x_{n-1} - s_{n-1}|$ with some $q \in (-\lambda, 1)$ independent of the point (x_{n-1}, s_{n-1}). In other words, since $x_n = \lambda x_{n-1} + a s_{n-1}$ and $s_n = -1$, we want to establish that

$$-(\lambda x_{n-1} + a s_{n-1} + 1) < (x_{n-1} - s_{n-1})q, \tag{4.10}$$

which is equivalent to

$$x_{n-1} - s_{n-1} > \frac{-\beta s_{n-1} - 1}{q + \lambda}.$$

Indeed, since the point (x_{n-1}, s_{n-1}) lies to the right of Π, we have $x_{n-1} - s_{n-1} > \frac{-a}{1-\lambda} + 1$ and it remains to show that

$$\frac{-a}{1-\lambda} + 1 > \frac{-\beta s_{n-1} - 1}{q + \lambda}.$$

This inequality is equivalent to

$$1 + q > -\beta s_{n-1}(1 - \lambda) + \beta(q + \lambda). \tag{4.11}$$

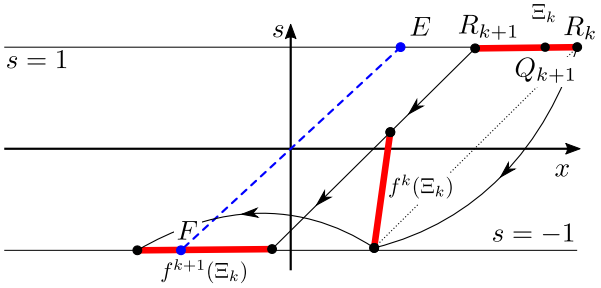

Figure 11. *The segment Ξ_k and its images $f^k(\Xi_k)$ and $f^{k+1}(\Xi_k)$.*

If we set $q = -\lambda + \varepsilon$ with a sufficiently small $\varepsilon > 0$, then $q \in (0,1)$ and the inequalities $|s_{n-1}| \le 1$ and $0 \le \beta < 1$ imply that

$$-\beta s_{n-1}(1-\lambda) < 1-\lambda, \qquad \beta(q+\lambda) = \varepsilon(\lambda+a) < \varepsilon,$$

hence the relation (4.11) holds.

Since q in (4.10) does not depend on (x_{n-1}, s_{n-1}) and the segment connecting the points $P_1 = (1,1)$ and $P_2 = (-1,-1)$ belongs to the interior of Π, all trajectories that start outside the parallelogram Π will eventually enter Π and converge to one of the equilibrium points.

4.6. Case (e). In this case, $a > 0$ and the slope of the segment EF is positive and less than 1 (see Figure 11). We divide the proof of this case into five parts.

1. We begin the proof of case (e) with a few definitions. Denote by l_1 and l_2 the open half-lines starting at the point E on the upper boundary of the strip L,

$$l_1 = \left\{(x,s) : x > \frac{a}{1-\lambda},\ s=1\right\}, \qquad l_2 = \left\{(x,s) : x < \frac{a}{1-\lambda},\ s=1\right\},$$

and by l_3 and l_4 the half-lines starting from the point F on the lower boundary of the strip L,

$$l_3 = \left\{(x,s) : x < -\frac{a}{1-\lambda},\ s=-1\right\}, \qquad l_4 = \left\{(x,s) : x > -\frac{a}{1-\lambda},\ s=-1\right\}.$$

From the condition $\lambda < 0$ it follows that $f(l_2) \subseteq l_1$ and $f(l_4) \subseteq l_3$. Also from Lemma 4.1 it follows that for any point (x_n, s_n) such that $x_n > \frac{as_n}{1-\lambda}$ one has $x_{n+1} < x_n$. Thus, starting from l_1, any trajectory arrives after finitely many iterations to the closed half-line $\overline{l_3}$. Hence, we can define the first-hitting map $\mathcal{P} : l_1 \to \overline{l_3}$ as $\mathcal{P}(A) = f^k(A)$, where $f^k(A) \in \overline{l_3}$ and $f^i(A) \notin \overline{l_3}$ for $i = 0, \dots, k-1$. This map can be represented by the scalar function $T : (\frac{a}{1-\lambda}, \infty) \to [\frac{a}{1-\lambda}, \infty)$ defined by the formula

$$(-T(x), -1) = \mathcal{P}(x, 1), \qquad x \in \left(\frac{a}{1-\lambda}, \infty\right). \tag{4.12}$$

It is convenient to set $T(\frac{a}{1-\lambda}) = \frac{a}{1-\lambda}$ and consider T as a map of the half-line $[\frac{a}{1-\lambda}, \infty)$ into itself.

2. In this part, we describe the structure of the function $T(x)$. We first make the following observation.

Lemma 4.7. *Let $(x_0, 1) \in l_1$ be a point such that the first $n-1$ iterations of it under the map f belong to the line $p = \text{const}$. Then for any $m \le n$ we have*

$$x_m = \beta^m x_0 - a(x_0 - 1)\sum_{i=0}^{m-1} \beta^i. \tag{4.13}$$

Proof. For $m = 1$, (4.13) is obvious. Suppose that (4.13) holds for $m < n$. Then

$$x_{m+1} = \lambda x_m + a(1 + x_m - x_0) = \beta^{m+1} x_0 - a(x_0 - 1)\sum_{i=0}^{m} \beta^i. \qquad \blacksquare$$

Let us show that for any $k \in \mathbb{N}$ there exists a unique point $(r_k, 1) \in l_1$ such that its first $k-1$ iterations under the map f belong to the line $p = \text{const}$ and its kth iteration is $(r_k - 2, -1)$. Setting $m = k$, $x_0 = r_k$, and $x_m = r_k - 2$ in (4.13), we obtain

$$r_k = \frac{2 + a\frac{1-\beta^k}{1-\beta}}{1 - \beta^k + a\frac{1-\beta^k}{1-\beta}} \tag{4.14}$$

(it is easy to see that the denominator does not vanish as long as $f^i(r_k, 1)$ belongs to the interior of L for $i = 1, \dots, k-1$).

Next we show that for any $k \in \mathbb{N}$ there exists a unique point $Q_k = (q_k, 1) \in l_1$ such that its first $k-1$ iterations under the map f belong to the line $p = \text{const}$ and its kth iteration is F.

Obviously, $q_1 = \frac{1}{\lambda}(-a - \frac{a}{1-\lambda})$. Set $R_i = (r_i, 1)$ and consider the kth iteration of the segment $\Xi_k = R_{k+1}R_k$. The point R_k is mapped to the point $(r_k - 2, -1)$, and the image of the point R_{k+1} belongs to the interior of L. Hence, $f^k(\Xi_k)$ is a segment which lies entirely to the right of the segment EF and all its points except $f^k(R_k)$ belong to the interior of L. Consider the $(k+1)$st iteration of Ξ_k. The point $f^{k+1}(R_k)$ lies on the line $s = -1$ to the left of the point F, while $f^{k+1}(R_{k+1}) = (r_{k+1} - 2, -1)$. Hence, $f^{k+1}(\Xi_k)$ is a segment on the line $s = -1$ and $F \in f^{k+1}(\Xi_k)$; see Figure 11. Hence, there exists a point $q_{k+1} \in (r_{k+1}, r_k)$ for each $k \in \mathbb{N}$. Now q_k can be found in a unique way using Lemma 4.7 by setting $m = k$, $x_0 = q_k$, and $x_m = \frac{-a}{1-\lambda}$:

$$q_k = \frac{-\frac{a}{1-\lambda} - a\frac{1-\beta^k}{1-\beta}}{\beta^k - a\frac{1-\beta^k}{1-\beta}}. \tag{4.15}$$

Since $\lambda < 0$ and $\beta > 1$, the denominator does not vanish. Note that

$$q_1 > r_1 > q_2 > r_2 > \cdots > \frac{a}{1-\lambda}, \qquad q_k, r_k \to \frac{a}{1-\lambda} \quad \text{as} \quad k \to \infty. \tag{4.16}$$

It follows from the relation $(r_k - 2, -1) = f^k(R_k)$ that $f^{k+1}(R_k) = (\lambda(r_k - 2) - a, -1)$, i.e.,

$$T(r_k) = a - \lambda(r_k - 2). \tag{4.17}$$

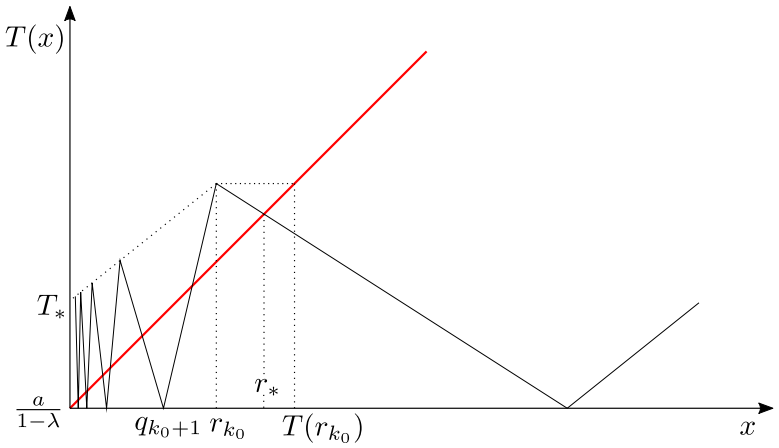

Figure 12. *Graph of the map $T(x)$ for $x \in (\frac{a}{1-\lambda}, \infty)$.*

Combining (4.16) and (4.17), we see that

$$\begin{aligned} &T(r_1) > T(r_2) > T(r_3) > \dots, \\ &T(r_k) - \frac{a}{1-\lambda} \to T_* > 0 \quad \text{as } k \to \infty, \end{aligned} \tag{4.18}$$

where

$$T_* = \frac{2\lambda(1-a-\lambda)}{1-\lambda}. \tag{4.19}$$

Furthermore, let us show that the function $T(x)$ is linear for $x \in [q_1, \infty)$, $x \in [q_{k+1}, r_k]$, and $x \in [r_k, q_k]$, $k = 1, 2, \dots$. This will imply that $T(x)$ is continuous for $x \in (a/(1-\lambda), \infty)$. Indeed, consider $x \in [q_{k+1}, r_k]$, i.e., $(x, 1) \in Q_{k+1}R_k \subset \Xi_k$ (see Figure 11). By (4.12) it suffices to show that $\mathcal{P}$ is affine linear on $Q_{k+1}R_k$. But $\mathcal{P}$ is a composition of k maps each of which is given by

$$\begin{cases} x_{n+1} = \lambda x_n + a s_n, \\ s_{n+1} = s_n + x_{n+1} - x_n \end{cases} \tag{4.20}$$

(see (2.2) with $\Phi(\tau) = \tau$) with the map

$$\begin{cases} x_{n+1} = \lambda x_n + a s_n, \\ s_{n+1} = -1 \end{cases} \tag{4.21}$$

(see (2.2) with $\Phi(\tau) = -1$). Since (4.20) and (4.21) are affine linear, so is $\mathcal{P}$. The cases $x \in [q_1, \infty)$ and $x \in [r_k, q_k]$ can be treated analogously.

Using (4.14), (4.15), and (4.17), we see that $T(x)$ increases on the intervals (q_1, ∞) and (q_k, r_{k-1}), $k = 2, 3, \dots$, with

$$T'(x) = -\lambda, \ x \in (q_1, \infty), \quad T'(x) = -\left(\beta^k - a\frac{1-\beta^k}{1-\beta}\right), \ x \in (q_k, r_{k-1}), \tag{4.22}$$

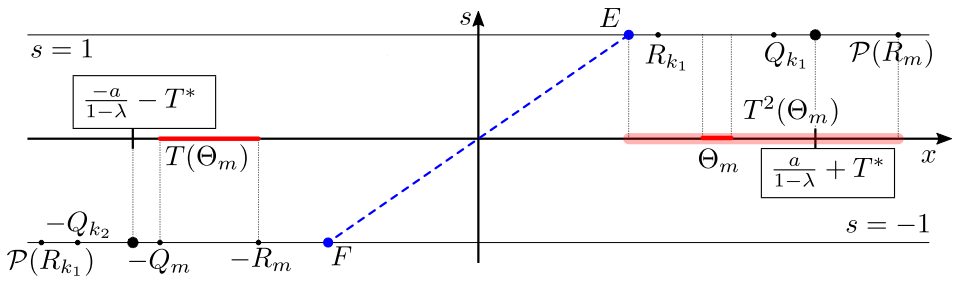

Figure 13. *Segment Θ_m is covered by its image $T^2(\Theta_m)$ under the second iteration of map T.*

respectively, and decreases on the intervals (r_k, q_k), $k \in \mathbb{N}$, with

$$T'(x) = -\lambda\left(\beta^k - a\frac{1-\beta^k}{1-\beta}\right), \quad x \in (r_k, q_k); \tag{4.23}$$

see Figure 12. Every point $x \in [q_1, \infty)$ possesses the property that $f(x, 1) \in l_3$. Every point $x \in [q_{k+1}, q_k)$, $k \in \mathbb{N}$, possesses the property that the $(k+1)$th iteration of the point $(x, 1) \in l_1$ under the map f reaches the half-line l_3 for the first time.

3. Now we show that system (2.2) has periodic orbits of all sufficiently large periods. Fix $k_1 \in \mathbb{N}$ such that

$$q_{k_1} - \frac{a}{1-\lambda} < T_*, \tag{4.24}$$

where $T_* > 0$ is given by (4.19).

Note that $T([r_{k_1}, q_{k_1}]) = [\frac{a}{1-\lambda}, T(r_{k_1})]$. Fix $k_2 \in \mathbb{N}$ such that

$$q_{k_2} < T(r_{k_1}).$$

For any $m \geq k_2$, denote by Θ_m the subsegment of $[r_{k_1}, q_{k_1}]$ such that $T(\Theta_m) = [r_m, q_m]$. It follows from (4.18) and (4.24) that

$$T^2(\Theta_m) \supset \left[\frac{a}{1-\lambda}, \frac{a}{1-\lambda} + T_*\right] \supset \Theta_m;$$

see Figure 13.

Hence, the map T^2 has a fixed point in Θ_m. Due to the argument in part 2 of this section, the corresponding periodic solution of the system (2.2) will be of period $k_1 + m + 2$. Hence, for any $k \geq k_1 + k_2 + 2$, system (2.2) has a k-periodic orbit.

4. To complete the proof of statement (e), it remains to show that system (2.2) has no more than one stable periodic orbit. In this part, we find a necessary and sufficient condition for the map $T(x)$ to have fixed points in the interval (q_{k+1}, q_k) (obviously, $T(x)$ has no fixed points for $x \geq q_1$ because $T'(x) = -\lambda \in (0, 1)$ for all $x > q_1$). Then we show that at most one fixed point of $T(x)$ can be stable. Finally, in part 5, we prove that all the periodic orbits of $T(x)$ with period greater than 1 are unstable.

Lemma 4.8. *The map $T(x)$ has a fixed point in the interval (q_{k+1}, q_k) if and only if*

$$1 + \lambda\beta^k \le 0. \tag{4.25}$$

The period of the corresponding orbit of system (2.2) equals $(2k + 2)$.

Proof. The interval (q_{k+1}, q_k) contains a fixed point if and only if

$$T(r_k) \ge r_k; \tag{4.26}$$

see Figure 12. Using formulas (4.14) and (4.17), we see that (4.26) is equivalent to

$$\frac{a + 2\lambda}{1 + \lambda} \ge \frac{2 + a\frac{1-\beta^k}{1-\beta}}{1 - \beta^k + a\frac{1-\beta^k}{1-\beta}},$$

which can be rewritten as (4.25). ∎

Note that, given a and λ, inequality (4.25) holds for all sufficiently large k. We denote by $k_0 = k_0(\lambda, a)$ the smallest k with this property.

Now we fix a and λ and an arbitrary $k \ge k_0(\lambda, a)$ and study the stability of the fixed points of $T(x)$ in the interval (q_{k+1}, q_k). First, note that if (4.25) holds as an equality, then the interval (q_{k+1}, q_k) contains a unique fixed point r_k. It is unstable because the slope of the graph of $T(x)$, $x \in (q_{k+1}, r_k)$ is positive and greater than one. Assume that (4.25) holds as a strict inequality, i.e.,

$$1 + \lambda\beta^k < 0. \tag{4.27}$$

Then there are two fixed points on the interval (q_{k+1}, q_k). The left one belongs to the interval $x \in (q_{k+1}, r_k)$ and is unstable (as in the previous case). The right one belongs to the interval (r_k, q_k). It is stable if and only if

$$T'(x) \in [-1, 0), \quad x \in (r_k, q_k). \tag{4.28}$$

Combining (4.28) and (4.23), we conclude that the fixed point from the interval (r_k, q_k) is stable if and only if

$$\lambda\beta^k + a - 1 \ge 0. \tag{4.29}$$

Lemma 4.9. *Inequalities (4.27) and (4.29) are either incompatible for all $k \ge k_0$ or they hold for $k = k_0$ only.*

Proof. In the parameter plane (λ, β), we introduce the regions Ω_k (see (2.8)). We proceed by contradiction. Assume that for given (λ, β), inequalities (4.27) and (4.29) hold for k_1 and k_2, $k_1 \ne k_2$. Then, $(\lambda, \beta) \in \Omega_{k_1} \cap \Omega_{k_2}$. But Ω_{k_1} and Ω_{k_2} do not intersect for $k_1 \ne k_2$. Hence, there exists no more than one $k \ge k_0$ for which inequalities (4.27) and (4.29) hold simultaneously. Now we again proceed by contradiction and assume that both inequalities hold for some $k > k_0$. Then inequality (4.27) holds also for k_0 by definition of k_0, while inequality (4.29) holds for k_0 due to the monotonicity of its left-hand side with respect to k. However, as we have just seen, both inequalities (4.27) and (4.29) cannot hold for two different values k and k_0 simultaneously. ∎

5. We denote by r_* the (unique) fixed point of the map $T(x)$ in the interval $[r_{k_0}, q_{k_0})$, where $k_0 = k_0(\lambda, a)$ was introduced in part 4. In this last part of the proof of case (e), it remains to show that all the fixed points of any iteration of $T(x)$, except for the possibly stable fixed point r_*, are unstable. Recall that the map $T(x)$ has no fixed points for $x > r_*$ (see Figure 12), which implies in particular

$$T(x) < x \quad \text{for all } x > r_*. \tag{4.30}$$

Now, let us show that the segment $[\frac{a}{1-\lambda}, T(r_{k_0})]$ is mapped onto itself under $T(x)$. Indeed, $[q_{k_0+1}, r_{k_0}] \subset [\frac{a}{1-\lambda}, T(r_{k_0})]$ and $T([q_{k_0+1}, r_{k_0}]) = [\frac{a}{1-\lambda}, T(r_{k_0})]$. Hence, $[\frac{a}{1-\lambda}, T(r_{k_0})] \subset T([\frac{a}{1-\lambda}, T(r_{k_0})])$. On the other hand, $T(x) \le T(r_{k_0})$ for $x \le r_*$ due to the monotonicity of $T(r_k)$ (see (4.18)) and $T(x) < x \le T(r_{k_0})$ for $x \in [r_*, T(r_{k_0})]$ due to (4.30). Thus,

$$T\left(\left[\frac{a}{1-\lambda}, T(r_{k_0})\right]\right) = \left[\frac{a}{1-\lambda}, T(r_{k_0})\right].$$

Further, we note that the fixed points of any iteration belong to the segment $[\frac{a}{1-\lambda}, T(r_{k_0})]$. Indeed, assume to the contrary that a fixed point x of some iteration of $T(x)$ satisfies $x > T(r_{k_0}) \ge r_*$. If $T^j(x) \in [\frac{a}{1-\lambda}, T(r_{k_0})]$ for some j, then all the subsequent iterations of $T^j(x)$ remain in the segment $[\frac{a}{1-\lambda}, T(r_{k_0})]$ due to the invariance of this segment. If $T^j(x) > T(r_{k_0})$ for all j, then (4.30) implies that $T^{j+1}(x) < T^j(x)$ for all j. In both cases, we obtain a contradiction with the fact that x is a fixed point of some iteration of $T(x)$.

We consider two cases: the fixed point r_* is stable or unstable.

5.1. Assume that the fixed point r_* is stable. Let us show that

$$T(r_{k_0}) \in [r_*, q_{k_0}). \tag{4.31}$$

Obviously $T(r_{k_0}) \ge r_*$. On the other hand, since

$$|T'(x)| \le 1 \quad \text{for all } x \in (r_{k_0}, q_{k_0}), \tag{4.32}$$

it follows that

$$q_{k_0} - r_{k_0} \ge T(r_{k_0}) - \frac{a}{1-\lambda} > T(r_{k_0}) - r_{k_0},$$

i.e., $T(r_{k_0}) \le q_{k_0}$.

Next, we show that the segment $[r_{k_0}, T(r_{k_0})]$ is invariant under T, i.e.,

$$T([r_{k_0}, T(r_{k_0})]) \subset [r_{k_0}, T(r_{k_0})]. \tag{4.33}$$

Since $T(x)$ is linear on this segment, we need to check the images $T(r_{k_0})$ and $T^2(r_{k_0})$ of the end points only. Obviously, $T(r_{k_0})$ belongs to this segment. Moreover, relations (4.31) and (4.32) show that all the iterations of r_{k_0} under the map T belong to the segment $[r_{k_0}, T(r_{k_0})]$ (and converge to r_*). In particular, $T^2(r_{k_0})$ belongs to this interval.

Now we are ready to prove that the fixed points of any iteration of $T(x)$, except for r_*, are unstable. Assume, to the contrary, that $x_* \in (\frac{a}{1-\lambda}, T(r_{k_0})]$ is a stable fixed point of $T^{j_*}(x)$ for some $j_* \ge 2$ and $x_* \ne r_*$. We have seen in part 4 of this section that $|T'(x)| > 1$ for all $x \in (r_{k+1}, q_{k+1}) \cup (q_{k+1}, r_k)$, $k \ge k_0$. Therefore, the only possibility for x_* to be stable is that $T^j(x_*) \in [r_{k_0}, T(r_{k_0})]$ for some $j \in \mathbb{N}$. However, all the trajectories entering this segment converge to r_* due to (4.32) and (4.33).

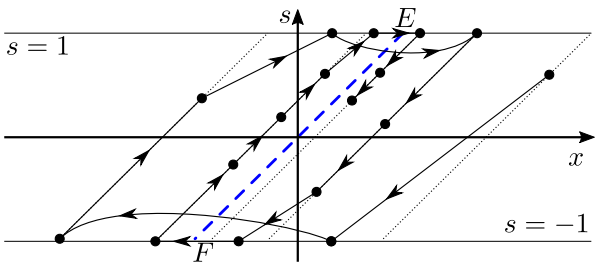

Figure 14. *Case $\beta = 1$, $\lambda < 0$. The parallelogram Π degenerates to the segment EF with slope 1.*

5.2. Assume that the fixed point r_* is unstable. Then $k_0 > 1$ (otherwise, $|T'(r_*)| = \lambda^2 < 1$). It follows from the monotonicity of $T(r_k)$ (see (4.18)) and (4.30) that $T(r_{k_0}) < T(r_{k_0-1}) < r_{k_0-1}$, i.e.,

$$\left[\frac{a}{1-\lambda}, T(r_{k_0})\right] \subset \left[\frac{a}{1-\lambda}, r_{k_0-1}\right]. \tag{4.34}$$

But $|T'(x)| > 1$ for all $x \in (q_{k+1}, r_k) \cup (r_k, q_k)$, $k \geq k_0$, due to part 4 of this section, and $|T'(x)| = |\lambda^{-1}T'(r_*)| > 1$ for all $x \in (q_{k_0}, r_{k_0-1})$ due to (4.22) and (4.23). This and (4.34) imply that the absolute values of all the slopes of the graph of $T(x)$ on the interval $[\frac{a}{1-\lambda}, T(r_{k_0})]$ are greater than 1. Hence, the same is true for any iteration of $T(x)$ on this interval. Therefore, all the fixed points of any iteration of T are unstable. This completes the proof of statement (e) of Theorem 2.1.

4.7. Case (f). In this case, the parallelogram Π degenerates into the segment of the equilibrium points EF with the slope 1 (see Figure 14).

Let us consider a point $(x_n, s_n) \notin EF$. To be definite, assume that $p_n = x_n - s_n > 0$. Denote by (x_{n+k}, s_{n+k}) the first iteration that reaches the line $s = -1$ after the moment n, i.e., $s_{n+i} > -1$ for $i = 0, \dots, k-1$ and $s_{n+k} = -1$ (if $s_n = -1$ we agree that $k = 0$). If $p_{n+k} = 0$, then the trajectory ends at the point F. If $p_{n+k} > 0$, then $0 < p_{n+k} \leq p_{n+k-1} = \dots = p_n$ and

$$p_{n+k+1} = \lambda x_{n+k} + a s_{n+k} - s_{n+k+1} = \lambda x_{n+k} - a + 1 = \lambda x_{n+k} + \lambda = \lambda p_{n+k}, \tag{4.35}$$

where we use $a = 1 - \lambda$. If $p_{n+k} < 0$, then $p_{n+k} < 0 < p_{n+k-1} = \dots = p_n$ and

$$p_{n+k} = \lambda x_{n+k-1} + a s_{n+k-1} - s_{n+k} = \lambda p_{n+k-1} + s_{n+k-1} - s_{n+k} \geq \lambda p_{n+k-1},$$

hence

$$|p_{n+k}| \leq |\lambda||p_{n+k-1}|. \tag{4.36}$$

Relations (4.35) and (4.36) and similar relations that hold for ascending parts of trajectories, due to (4.1), show that the trajectory either ends up at E or F or converges to the segment EF. In the latter case, the distance from the point (x_n, s_n) to the segment EF tends to zero as $n \to \infty$.

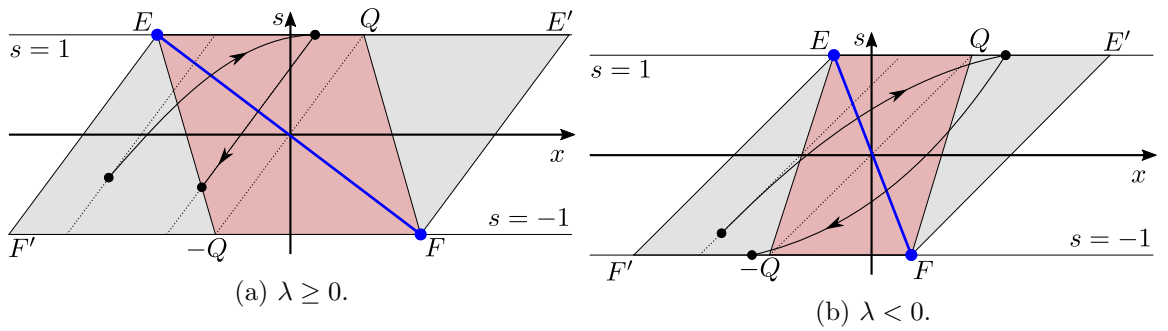

(a) $\lambda \geq 0$. (b) $\lambda < 0$.

Figure 15. *Parallelograms* Σ *and* Π *for* $\beta = -1$.

4.8. Case (g). For $\beta = -1$ it is straightforward to see that the parallelogram Σ, which is contained in Π, consists of 2-periodic orbits and the segment EF of equilibrium points.

If $\lambda \geq 0$ (see Figure 15(a)), then from Lemma 4.4 it follows that the parallelogram Π is invariant under the map f, and if $(x_n, s_n) \in \Pi \setminus \Sigma$, then either $(x_{n+1}, s_{n+1}) \in \Sigma$ or $x_{n+1} < -1$, $s_{n+1} = -1$ or $x_{n+1} > 1$, $s_{n+1} = 1$. But, since $\lambda \geq 0$, relations $x_{n+1} < -1$, $s_{n+1} = -1$, and $f(-1,-1) = (1,1)$ imply $x_{n+2} < 1$, $s_{n+2} = 1$ and, similarly, relations $x_{n+1} > 1$, $s_{n+1} = 1$, and $f(1,1) = (-1,-1)$ imply $x_{n+2} > -1$, $s_{n+2} = -1$. In both cases, $(x_{n+2}, s_{n+2}) \in \Sigma$. Thus, f^2 maps Π into Σ. On the other hand, the same argument as the one presented in section 4.3.5 shows that a trajectory starting outside Π either converges to the point F along the line $s = -1$ from the right or to the point E along the line $s = 1$ from the left or meets the boundary of the strip L inside Π.

If $\lambda < 0$ (see Figure 15(b)), then the argument used in section 4.4 shows that the set $M = \{(x,s) : x \leq -1, s = -1\} \cup \{(x,s) : x \geq 1, s = 1\}$ is invariant under the map f and all the trajectories starting in M converge to the 2-periodic orbit $(-1,-1)$, $(1,1)$. If $(x_n, s_n) \in \Pi \setminus \Sigma$, then $(x_{n+1}, s_{n+1}) \in M \cup \Sigma$ because $\beta = -1$. Finally, if $(x_n, s_n) \notin \Pi$, then $(x_{n+k}, s_{n+k}) \in M \cup \Sigma$ for some $k \in \mathbb{N}$. This completes the proof of Theorem 2.1.

Proof of Theorem 2.2. We use the notation of section 4.6. If $(\lambda, \beta) \in \Omega_k$ for some $k \in \mathbb{N}$, then, according to Lemmas 4.8 and 4.9, the map T has a stable fixed point in the interval $[r_k, q_k)$ and $k = k_0(\lambda, a)$. It corresponds to the stable $(2k+2)$-periodic orbit of system (2.2). According to part 5.1 of this section, all the other periodic orbits are unstable.

If $(\lambda, a) \notin \bigcup_{k \in \mathbb{N}} \Omega_k$, then, according to Lemma 4.9, the map T has no stable fixed points. Therefore, due to part 5.2 of this section, all the periodic orbits are unstable.

5. Conclusions. We have studied the discrete time dynamics of the simplest closed loop system that includes a linear unit and a stop operator. This system can be equivalently represented as a two-dimensional piecewise linear map involving a scalar-valued saturation function. We have obtained a two-dimensional bifurcation diagram, which describes global dynamics depending on two parameters. It should be noted that the system has a segment of equilibrium points for every set of parameter values. The global attractor of the system may have different forms: the segment of equilibrium points; the two equilibrium points at the ends of this segment; a 2-periodic orbit; a 2-periodic orbit together with two equilibrium points. The 2-periodic orbit is generated via a type of border-collision degenerate flip bifurcation. For

certain parameter values the system has either a global chaotic attractor or a locally stable periodic orbit coexisting with a chaotic set. We have also shown numerically that higher-dimensional systems with a stop operator can demonstrate similar dynamics. Such systems may be motivated by mechanical and economic applications.

REFERENCES

[1] F. Al-Bender, W. Symens, J. Swevers, and H. Van Brussel, *Theoretical analysis of the dynamic behavior of hysteresis elements in mechanical systems*, Internat. J. Non-Linear Mech., 39 (2004), pp. 1721–1735.

[2] B. Appleby, D. Flynn, H. Mcnamara, P. O'Kane, A. Pimenov, A. Pokrovskii, D. Rachinskii, and A. Zhezherun, *Rate-independent hysteresis in terrestrial hydrology*, IEEE Trans. Control Systems, 29 (2009), pp. 44–69.

[3] B. Appleby, D. Rachinskii, and A. Zhezherun, *Hopf bifurcation in a Van der Pol type oscillator with magnetic hysteresis*, Phys. B, 403 (2008), pp. 301–304.

[4] K. J. Åström, *Oscillations in systems with relay feedback*, in Adaptive Control, Filtering, and Signal Processing (Minneapolis, MN, 1993), IMA Vol. Math. Appl. 74, Springer, New York, 1995, pp. 1–25, http://dx.doi.org/10.1007/978-1-4419-8568-2_1.

[5] Z. Balanov, W. Krawcewicz, D. Rachinskii, and A. Zhezherun, *Hopf bifurcation in symmetric networks of coupled oscillators with hysteresis*, J. Dynam. Differential Equations, 24 (2012), pp. 713–759, http://dx.doi.org/10.1007/s10884-012-9271-4.

[6] L. M. Ball, *Hysteresis in Unemployment: Old and New Evidence*, Tech. report, National Bureau of Economic Research, 2009.

[7] J. Barrdear, *Towards a New Keynesian Theory of the Price Level*, Tech. report, Bank of England and the Centre for Macroeconomics, 2015.

[8] A. Belke, M. Göcke, and M. Günther, *Exchange rate bands of inaction and play-hysteresis in German exports: Sectoral evidence for some OECD destinations*, Metroeconomica, 64 (2013), pp. 152–179.

[9] J. Bellaïche, *On the path-dependence of economic growth*, J. Math. Econom., 46 (2010), pp. 163–178, http://dx.doi.org/10.1016/j.jmateco.2009.11.002.

[10] M. Brokate, S. McCarthy, A. Pimenov, A. Pokrovskii, and D. Rachinskii, *Energy dissipation in hydrological due to hysteresis*, Environ. Model. Assess., 16 (2011), pp. 313–333.

[11] M. Brokate, A. Pokrovskii, D. Rachinskii, and O. Rasskazov, *Differential equations with hysteresis via a canonical example*, in The Science of Hysteresis, G. Bertotti and I. Mayergoyz, eds., Academic Press, Oxford, UK, 2006, pp. 127–291.

[12] M. Brokate and J. Sprekels, *Hysteresis and Phase Transitions*, Springer-Verlag, New York, 1996.

[13] L. Christiano, M. Trabandt, and K. Walentin, *DSGE models for monetary policy analysis*, in Handbook of Monetary Economics, Elsevier, New York, 2011, pp. 285–367.

[14] R. Cross, M. Grinfeld, H. Lamba, and T. Seaman, *Stylized facts from a threshold-based heterogeneous agent model*, Eur. Phys. J. B, 57 (2007), pp. 213–218, http://dx.doi.org/10.1140/epjb/e2007-00108-5.

[15] R. Cross, H. Hutchinson, H. Lamba, and D. Strachan, *Reflections on Soros: Mach, Quine, Arthur and far-from-equilibrium dynamics*, J. Econom. Methodology, 20 (2013), pp. 357–367.

[16] R. Cross, H. McNamara, A. Pokrovskii, and D. Rachinskii, *A new paradigm for modelling hysteresis in macroeconomic flows*, Phys. B, 403 (2008), pp. 231–236.

[17] J. Darby, R. Cross, and L. Piscitelli, *Hysteresis and unemployment: A preliminary investigation*, in The Science of Hysteresis, G. Bertotti and I. D. Mayergoyz, eds., Academic Press, Oxford, UK, 2006, pp. 667–699.

[18] D. Davino, P. Krejčí, and C. Visone, *Fully coupled modeling of magneto-mechanical hysteresis through thermodynamic compatibility*, Smart Materials Structures, 22 (2013), 095009.

[19] P. De Grauwe, *Booms and busts in economic activity: A behavioral explanation*, J. Econom. Behavior Organization, 83 (2012), pp. 484–501.

[20] J. C. Driscoll and S. Holden, *Behavioral economics and macroeconomic models*, J. Macroeconomics, 41 (2014), pp. 133–147.
[21] M. Eleuteri, J. Kopfova, and P. Krejčí, *A new phase field model for material fatigue in an oscillating elastoplastic beam*, Discrete Contin. Dyn. Syst., 35 (2015), pp. 2465–2495, http://dx.doi.org/10.3934/dcds.2015.35.2465.
[22] D. Fournier-Prunaret, P. Chargé, and L. Gardini, *Border collision bifurcations and chaotic sets in a two-dimensional piecewise linear map*, Comm. Nonlinear Sci. Numer. Simul., 16 (2011), pp. 916–927.
[23] G. Friedman, S. McCarthy, and D. Rachinskii, *Hysteresis can grant fitness in stochastically varying environment*, PloS ONE, 9 (2014), e103241.
[24] L. Gardini, D. Fournier-Prunaret, and P. Chargé, *Border collision bifurcations in a two-dimensional piecewise smooth map from a simple switching circuit*, Chaos, 21 (2011), 023106.
[25] M. Göcke, *Various concepts of hysteresis applied in economics*, J. Econom. Surveys, 16 (2002), pp. 167–188.
[26] M. Göcke and L. Werner, *Play hysteresis in supply or in demand as part of a market model*, Metroeconomica, 66 (2015), pp. 339–374.
[27] R. S. Harris, *Pressure-volume curves of the respiratory system*, Respiratory Care, 50 (2005), pp. 78–99.
[28] N. Hinrichs, M. Oestreich, and K. Popp, *On the modelling of friction oscillators*, J. Sound Vibration, 216 (1998), pp. 435–459.
[29] R. V. Iyer and X. Tan, *Control of hysteretic systems through inverse compensation*, IEEE Control Syst. Mag., 29 (2009), pp. 83–99, http://dx.doi.org/10.1109/MCS.2008.930924.
[30] M. A. Janaideh, S. Rakheja, and C.-Y. Su, *A generalized Prandtl–Ishlinskii model for characterizing the hysteresis and saturation nonlinearities of smart actuators*, Smart Materials Structures, 18 (2009), 045001.
[31] B. Jayawardhana, R. Ouyang, and V. Andrieu, *Stability of systems with the Duhem hysteresis operator: the dissipativity approach*, Automatica J. IFAC, 48 (2012), pp. 2657–2662, http://dx.doi.org/10.1016/j.automatica.2012.06.069.
[32] B. D. Keen, *Output, inflation, and interest rates in an estimated optimizing model of monetary policy*, Rev. Econom. Dynam., 12 (2009), pp. 327–343.
[33] A. Krasnosel'skii and D. Rachinskii, *Bifurcation of forced periodic oscillations for equations with Preisach hysteresis*, J. Phys. Conf. Ser., 22 (2005), pp. 93–102.
[34] M. A. Krasnosel'skii and A. V. Pokrovskii, *Systems with Hysteresis*, Springer-Verlag, Berlin, 1989.
[35] P. Krejčí, *Hysteresis, Convexity and Dissipation in Hyperbolic Equations*, Gakkōtosho, Tokyo, 1996.
[36] P. Krejčí, H. Lamba, S. Melnik, and D. Rachinskii, *Analytical solution for a class of network dynamics with mechanical and financial applications*, Phys. Rev. E, 90 (2014), 032822.
[37] P. Krejčí, J. P. O'Kane, A. Pokrovskii, and D. Rachinskii, *Stability results for a soil model with singular hysteretic hydrology*, J. Phys. Conf. Ser., 268 (2011), 012016.
[38] P. Krejčí and J. Sprekels, *Elastic-ideally plastic beams and Prandtl-Ishlinskii hysteresis operators*, Math. Methods Appl. Sci., 30 (2007), pp. 2371–2393, http://dx.doi.org/10.1002/mma.892.
[39] P. Krejči, *Forced oscillations in Preisach systems*, Phys. B, 275 (2000), pp. 81–86.
[40] M. Kunze and M. D. P. Monteiro Marques, *an introduction to Moreau's sweeping process*, in Impacts in Mechanical Systems (Grenoble, 1999), Lecture Notes in Phys. 551, Springer, Berlin, 2000, pp. 1–60, http://dx.doi.org/10.1007/3-540-45501-9_1.
[41] H. Lamba, *Implausible Equilibrium Solutions in Economics and Finance*, SSRN 2408013, 2014.
[42] H. Lamba and T. Seaman, *Market statistics of a psychology-based heterogeneous agent model*, Int. J. Theor. Appl. Finance, 11 (2008), pp. 717–737.
[43] Y. L. Maistrenko, V. L. Maistrenko, and L. O. Chua, *Cycles of chaotic intervals in a time-delayed chuas circuit*, Int. J. Bifurcation Chaos, 3 (1993), pp. 1557–1572.
[44] M. G. Mankiw and R. Reis, *Sticky information versus sticky prices: A proposal to replace the new Keynesian Phillips curve*, Quart. J. Economics, 117 (2002), pp. 1295–1328, http://www.jstor.org/stable/4132479.
[45] N. G. Mankiw and R. Reis, *Sticky information in general equilibrium*, J. European Economic Association, 5 (2007), pp. 603–613.
[46] I. D. Mayergoyz, *Mathematical Models of Hysteresis and Their Applications*, Electromagnetism, Elsevier Science, New York, 2003.

[47] J.-J. Moreau, *On unilateral constraints, friction and plasticity*, in New Variational Techniques in Mathematical Physics (Centro Internaz. Mat. Estivo (C.I.M.E.), II Ciclo, Bressanone, 1973), Edizioni Cremonese, Rome, 1974, pp. 171–322.

[48] J.-Y. Parlange, R. Haverkamp, G. Sander, W. L. Hogarth, and R. D. Braddock, *Comments on "General scaling rules of the hysteretic water retention function based on Mualem's domain theory" by Y. Mualem & A. Beriozkin*, European J. Soil Sci., 61 (2010), pp. 1113–1114.

[49] L. Prandtl, *Ein Gedankenmodell zur kinetischen Theorie der festen Körper*, ZAMM Z. Angew. Math. Mech., 8 (1928), pp. 85–106.

[50] K. Rao, A. M. Sbordone, A. Tambalotti, and K. J. Walsh, *Policy analysis using DSGE models: An introduction*, Economic Policy Rev., 16 (2010).

[51] M. Ruderman, *Presliding hysteresis damping of LuGre and Maxwell slip friction models*, Mechatronics, 30 (2015), pp. 225–230.

[52] M. Ruderman and T. Bertram, *Modified Maxwell-slip model of presliding friction*, in Proceedings of the 18th IFAC World Congress, 2011, pp. 10764–10769.

[53] I. Rychlik, *A new definition of the rainflow cycle counting method*, Internat. J. Fatigue, 9 (1987), pp. 119–121.

[54] T. C. Schelling, *Dynamic models of segregation*, J. Math. Sociol., 1 (1971), pp. 143–186.

[55] D. J. W. Simpson and J. D. Meiss, *Neimark-Sacker bifurcations in planar, piecewise-smooth, continuous maps*, SIAM J. Appl. Dyn. Syst., 7 (2008), pp. 795–824.

[56] I. Sushko and L. Gardini, *Center bifurcation for a two-dimensional border-collision normal form*, Int. J. Bifurcation Chaos, 18 (2008), pp. 1029–1050.

[57] I. Sushko and L. Gardini, *Degenerate bifurcations and border collisions in piecewise smooth* $1d$ *and* $2d$ *maps*, Int. J. Bifurcation Chaos, 20 (2010), pp. 2045–2070.

[58] J. B. Taylor, *The inflation/output variability trade-off revisited*, in Goals, Guidelines and Constraints Facing Monetary Policymakers, Conference Ser. 38, Federal Reserve Bank of Boston, 1994, pp. 21–38.

[59] A. Visintin, *Differential Models of Hysteresis*, Appl. Math. Sci., Springer, Berlin, 1994.

[60] P. P. Zabreiko, M. A. Krasnosel'skii, and E. A. Lifsic, *An oscillator on an elasto-plastic element*, Dokl. Akad. Nauk SSSR, 190 (1970), pp. 266–268.